

# Sleep Spindle-dependent Functional Connectivity Correlates with Cognitive Abilities

Zhuo Fang<sup>1,2</sup>, Laura B. Ray<sup>1,2</sup>, Evan Houldin<sup>1</sup>, Dylan Smith<sup>2</sup>,  
Adrian M. Owen<sup>1</sup>, and Stuart M. Fogel<sup>1,2</sup>

## Abstract

■ EEG studies have shown that interindividual differences in the electrophysiological properties of sleep spindles (e.g., density, amplitude, duration) are highly correlated with trait-like “reasoning” abilities (i.e., “fluid intelligence”; problem-solving skills; the ability to employ logic or identify complex patterns), but not interindividual differences in STM or “verbal” intellectual abilities. Previous simultaneous EEG-fMRI studies revealed brain activations time-locked to spindles. Our group has recently demonstrated that the extent of activation in a subset of these regions was related to interindividual differences in reasoning intellectual abilities, specifically. However, spindles reflect communication between spatially distant and functionally distinct brain areas. The functional communication among brain regions related to spindles and their relationship to reasoning abilities

have yet to be investigated. Using simultaneous EEG-fMRI sleep recordings and psychophysiological interaction analysis, we identified spindle-related functional communication among brain regions in the thalamo-cortical-BG system, the salience network, and the default mode network. Furthermore, the extent of the functional connectivity of the cortical–striatal circuitry and the thalamo-cortical circuitry was specifically related to reasoning abilities but was unrelated to STM or verbal abilities, thus suggesting that individuals with higher fluid intelligence have stronger functional coupling among these brain areas during spontaneous spindle events. This may serve as a first step in further understanding the function of sleep spindles and the brain network functional communication, which support the capacity for fluid intelligence. ■

## INTRODUCTION

Sleep spindles are brief oscillatory events that appear in the EEG during non-rapid eye movement (NREM) sleep. They have a “waxing” and “waning” amplitude envelope and oscillate in the frequency range of ~11–16 Hz. Spindles last up to ~3 sec and occur approximately every 1–10 sec throughout NREM sleep (Iber, Ancoli-Israel, Chesson, & Quan, 2007). The neural substrates and generating mechanisms of spindle production have been extensively studied in a variety of mammalian species, initially via electrophysiology (Steriade, 2006; Steriade, McCormick, & Sejnowski, 1993; Steriade, Domich, Oakson, & Deschênes, 1987) and computational methods (Bonjean et al., 2012; Destexhe & Sejnowski, 2003; Timofeev, 2001) and, more recently, in combination with molecular imaging approaches (Luthi, 2014). Converging evidence from these studies have shown that the thalamus is the main hub of oscillatory spindle generation, with widespread connections to functionally diverse cortical and subcortical regions. Nonetheless, a complex interplay between neocortical and thalamic regions occurs during spindle propagation. Specifically, during spindle initiation and termination, thalamo-cortical input

initiates spindle events by triggering spike bursts in the reticular nucleus, which are then terminated by desynchronization of thalamic and cortical neuronal firing (Bonjean et al., 2011, 2012), thereby suggesting that spindles are more cortically driven than originally thought. However, the extent of the dynamics within this network of brain regions involved in the production of spindle events, and importantly, the functional significance of this communication between these brain regions, remains to be investigated.

Recently, using simultaneous EEG and fMRI (EEG-fMRI), a handful of studies have explored brain activations time-locked to spindles (Fogel, Albouy, et al., 2017; Bergmann, Mölle, Diedrichs, Born, & Siebner, 2012; Caporro et al., 2012; Andrade et al., 2011; Tyvaert, Levan, Grova, Dubeau, & Gotman, 2008; Laufs, Walker, & Lund, 2007; Schabus et al., 2007). These studies have consistently revealed spindle-related activations in the thalamus and the temporal lobe. In addition, activation of the cingulate cortex, motor areas (Caporro et al., 2012; Andrade et al., 2011), and the putamen (Caporro et al., 2012; Tyvaert et al., 2008) has also been found to be associated with spindles. These neuroimaging studies, in line with previous physiological animal studies, provide converging support for the role of the thalamus and neocortex in spindle generation.

<sup>1</sup>Western University, London, Canada, <sup>2</sup>University of Ottawa

Interestingly, these studies also revealed an association between spindles and the activation of brain regions that are critically involved in human memory and cognitive abilities including the BG (Fogel et al., 2017; Caporro et al., 2012; Tyvaert et al., 2008) and parahippocampus (Schabus et al., 2007). However, no studies have investigated how interindividual differences in brain functional connectivity (FC) recruited during spindle events relate to interindividual differences in cognitive abilities.

Converging evidence from a number of cognitive and electrophysiological studies (Fang et al., 2017; Ujma et al., 2014, 2015; Bódizs, Lázár, & Rigó, 2008; Fogel, Nader, Cote, & Smith, 2007; Schabus et al., 2006; Bódizs et al., 2005; Nader & Smith, 2001, 2003) have consistently shown that the considerable interindividual variability in sleep spindles (De Gennaro, Ferrara, Vecchio, Curcio, & Bertini, 2005; Silverstein & Levy, 1976) is highly correlated with human cognitive abilities (typically assessed using neuropsychological tests, such as intelligence quotient [IQ] tests). Specifically, these studies have shown that spindles are specifically related to cognitive capabilities that reflect the ability to identify complex patterns and relationships and the use of logic, skills, and experience to solve novel problems. This distinct set of cognitive abilities has been synonymously referred to as “reasoning” abilities (Yuan et al., 2012; Kalbfleisch, Van Meter, & Zeffiro, 2007), “fluid intelligence” (Salthouse, Pink, & Tucker-Drob, 2008; Tranter & Koutstaal, 2008; Kanazawa, 2004), and “performance IQ” (Fogel et al., 2007; Jackson, 1998). Moreover, previous work has shown that, when accounting for the overlap between these various cognitive subdomains (Fang et al., 2017; Fogel et al., 2007), spindles are not associated with the set of cognitive abilities collectively referred to as “verbal abilities,” “crystallized intelligence,” or “verbal IQ,” which reflect the ability to use and remember facts, figures, events, and places (Schipolowski, Wilhelm, & Schroeders, 2014; Beauducel, Brocke, & Liepmann, 2001; Sternberg, Conway, Ketrone, & Bernstein, 1981). Similarly, interindividual differences in spindles are not associated with the ability to maintain and manipulate information in STM. Thus, spindles appear to be uniquely related to reasoning, but not verbal abilities or STM.

Using simultaneous EEG-fMRI, our group has recently demonstrated that the extent of activation within a subset of brain regions recruited during spontaneous spindle events is correlated with reasoning, but not STM or verbal abilities (Fang, Ray, Owen, & Fogel, 2019). Interestingly, many of the brain regions activated during spindles, including regions that comprise thalamo-cortical circuitry (i.e., the PFC, the thalamus, and the BG), have also been found to be activated when performing tasks that test reasoning abilities, such as the Raven’s Standard Progressive Matrices (Melrose, Poulin, & Stern, 2007; Gray, Chabris, & Braver, 2003; Waltz et al., 1999) as well as other reasoning-related tasks (Rodriguez-Moreno & Hirsch, 2009; Melrose et al., 2007). Thus, evidence

suggests that individuals who show stronger activation of brain regions recruited during spindle events have greater reasoning abilities when compared with individuals who show less activation of spindle-associated regions. However, scalp-recorded spindles are inherently oscillatory events and reflect communication between disparate brain regions (e.g., thalamo-cortical circuitry). Therefore, the magnitude of functional communication within and between brain regions recruited during spindle events may relate to reasoning abilities, although no studies to date have investigated how interindividual differences in brain FC recruited during spindle events relate to interindividual differences in cognitive abilities. The investigation of this relationship may reveal communication nodes that support specific intellectual abilities and provide neurophysiological evidence to suggest that spindles are a biomarker of intellectual functioning.

Several studies, using EEG and MEG, have explored brain connectivity related to spindles (Boutin et al., 2018; Das et al., 2017; Cox, van Driel, de Boer, & Talamini, 2014; Zerouali et al., 2014). Notably, EEG recordings and BOLD time courses are inherently different signals, measuring different types of brain activity. Accordingly, EEG and fMRI data are processed differently, and the algorithms used to assess FC of these two data types are distinct from one another (Wirsich et al., 2017; Deligianni, Centeno, Carmichael, & Clayden, 2014). As an example, a previous study compared fMRI connectivity and connectivity derived from EEG (Deligianni et al., 2014) and has shown that, although EEG connectomes are similar to fMRI connectomes in cortical regions, they are dissimilar in subcortical regions. Because scalp-recorded EEG derives its signal from cortical regions, this is perhaps unsurprising. Although some converging evidence would be expected between these very different but complimentary modalities, a 1:1 region-by-region correspondence would not be expected. To our knowledge, the study of Andrade et al. (2011) is the only study that has previously investigated FC specific to spindle events using simultaneous EEG-fMRI; however, they did not examine the relationship between the spindle-dependent FC and interindividual differences in intellectual abilities. Consequently, using a unique combination of cognitive testing, simultaneous EEG-fMRI during sleep, we sought to investigate which networks of brain regions communicate with one another during sleep spindle events and to what extent this communication is related to reasoning abilities.

More specifically, using the seed-based psychophysiological interaction (PPI) analysis approach, we aim to explore fMRI-based FC time-locked to spindles and its relationship to interindividual differences in reasoning, verbal, and STM abilities. On the basis of previous literature, this investigation focused on the following ROIs: (1) the thalamus and PFC region, part of the thalamo-cortical circuitry involved in spindle production (Caporro et al., 2012; Andrade et al., 2011; Tyvaert et al., 2008; Laufs

et al., 2007; Schabus et al., 2007); (2) the putamen (Fang et al., 2017; Caporro et al., 2012; Tyvaert et al., 2008); (3) the posterior cingulate cortex (PCC), i.e., the central node of the default mode network (DMN), which has been reported to be recruited during light NREM Stage 2 sleep (NREM2) when spindles predominate (Horovitz et al., 2009; Larson-Prior et al., 2009); and (4) hippocampus, which has been shown to be time-locked to spindles and has been suggested to support memory consolidation during sleep (Clemens et al., 2007, 2011; Girardeau & Zugaro, 2011). Using this approach, we expected to reveal the functionally connected networks of brain regions, which are recruited during spindle events, that support human cognitive abilities during sleep. More specifically, we hypothesized that spindle-related FC within the thalamo-cortical-BG circuitry, which has been reported to be involved in both spindle generation (Bonjean et al., 2011, 2012; Steriade, 2006; Steriade, McCormick, et al., 1993; Steriade et al., 1987) and to support cognitive processes (Melrose et al., 2007; Gray et al., 2003; Waltz et al., 1999), would be related to inter-individual differences in human intellectual abilities, particularly reasoning abilities, but not STM or verbal abilities.

## METHODS

### Participants

A total of 35 healthy, right-handed adults (20 women) between 20 and 35 years ( $M = 23.69$ ,  $SD = 3.57$ ) were recruited to participate in this study. All participants were nonshift workers; were medication free; had no history of head injury or seizures; had a normal body mass index ( $< 25$ ); and did not consume excessive caffeine, nicotine, or alcohol. To be included, interested participants had to score  $< 10$  on the Beck Depression (Beck, Rial, & Rickels, 1974) and Beck Anxiety Inventories (Beck, AaronSteer, & Carbin, 1988) and have no history or signs of sleep disorders indicated by the Sleep Disorders Questionnaire (Douglass et al., 1994). Extreme morning and evening types were excluded based on the Morningness-Eveningness Questionnaire (Horne & Ostberg, 1976). All participants were required to keep a regular sleep-wake schedule (bedtime between 22:00 and 24:00, wake time between 07:00 and 09:00) and to abstain from taking daytime naps at least 7 days before and throughout participation in the study. Compliance with this schedule was assessed using both sleep diaries and wrist actigraphy (Actiwatch 2, Philips Respironics). All participants were required to meet MRI safety screening criteria. In addition, participants were given a letter of information, provided informed written consent before participation, and were financially compensated for their participation. All study procedures and methods adhered to the Declaration of Helsinki and were approved by the Western University Health Science Research Ethics Board.

To be included in the analyses, participants were required to sleep for a period of at least 5 min of uninterrupted NREM sleep during the EEG-fMRI sleep session. This was considered to be the absolute minimum amount of data necessary for EEG and fMRI data analysis purposes and to ensure a minimum duration, quality, and continuity of sleep. Of the 35 participants who met the inclusion criteria, only five participants did not meet the minimum 5-min consolidated NREM sleep criteria for the EEG-fMRI sleep session. As well, one participant did not complete the cognitive ability test battery. In total,  $N = 29$  participants ( $M = 23.97$ ,  $SD = 3.83$ , 17 women) were included in the final data analyses. It should be noted that all 29 participants included had more than 14.67 min of sleep, with a minimum of 63 spindle events. Importantly, the average duration of NREM sleep in the MRI scanner was 39.29 min, with an average of 334.74 spindles. The detailed sleep architecture and sleep spindle parameters are reported in Table 1. All participants were normally rested and did not undergo sleep deprivation before the EEG-fMRI sleep session.

The necessary sample size was determined a priori based on previous studies, and power was calculated, where possible, using G\*Power for Mac Version 3.1 (Faul, Erdfelder, Buchner, & Lang, 2009; Faul, Erdfelder, Lang, & Buchner, 2007). On the basis of the most comparable simultaneous EEG-fMRI studies (Caporro et al., 2012; Andrade et al., 2011; Tyvaert et al., 2008; Laufs

**Table 1.** Sleep Architecture and Spindle Parameters for Spindles during NREM Sleep from EEG-fMRI Recording Sessions

|                           | Mean Value | SD     |
|---------------------------|------------|--------|
| <i>Sleep Architecture</i> |            |        |
| Wake (min) ( $N = 26$ )   | 26.87      | 20.25  |
| NREM1 (min) ( $N = 26$ )  | 5.84       | 4.38   |
| NREM2 (min) ( $N = 29$ )  | 23.87      | 14.5   |
| SWS (min) ( $N = 20$ )    | 14.77      | 17.17  |
| NREM (min)                | 39.29      | 19.33  |
| REM ( $N = 8$ )           | 17.8       | 10.76  |
| Total sleep (min)         | 44.2       | 23.84  |
| Sleep latency             | 8.16       | 10.11  |
| <i>Spindle Parameters</i> |            |        |
| Number                    | 334.74     | 212.29 |
| Duration (sec)            | 0.49       | 0.05   |
| Amplitude ( $\mu$ V)      | 27.21      | 6.43   |
| Density (#/min)           | 8.22       | 2.34   |

NREM1 = Stage 1 sleep; NREM2 = Stage 2 sleep.

et al., 2007; Schabus et al., 2007), previous studies have employed sample sizes of  $N < 15$ . A recent study by our group using the same cognitive tests as the current study (Fang et al., 2017) found robust associations between spindles and cognitive abilities in a sample size of  $N = 24$ , replicating previous findings in smaller samples (e.g.,  $N < 12$ : Fogel et al., 2007; Fogel & Smith, 2006). On the basis of power calculations for correlation with  $p$  (two-tailed) = .05 ( $b = 0.20$ , effect size = 0.56; Fang et al., 2017), an  $N = 22$  was required. Thus, the  $N = 29$  participants included in this study was considered to provide adequate statistical power for the main effects of interest.

## Experimental Procedure

The experimental procedure is shown in Figure 1. Participants underwent an initial screening session before inclusion in the study by completing the Sleep Disorders Questionnaire, Beck Depression Inventory, Beck Anxiety Inventory, Horne–Ostberg Morningness-Eveningness Questionnaire, and an MRI safety questionnaire to screen for signs of sleep disorders, unusual sleep habits, depression or anxiety, and MRI compatibility. Eligible participants underwent an orientation session, during which participants were given the instruction for the study, a guide to complete the online cognitive ability tests, a sleep diary, and an actiwatch to verify their sleep–wake cycle. After the orientation session, participants completed the online cognitive ability tests. During the EEG–fMRI sleep recording night, the scanning session was conducted between 21:00 and 24:00, at the end of which simultaneous EEG–fMRI was recorded while participants slept in the scanner. Specifically, the scan procedure

started at 21:00, at which point, the EEG equipment was installed and tested. This was followed by localizer scans, a T1 magnetization prepared rapid gradient echo structural scan, and an 8-min eyes-closed awake resting-state scan, where EEG was also acquired and used to confirm that participants were awake, scored in accordance with standard criteria (Iber et al., 2007). These procedures took up to an hour to complete. The sleep recording (“lights out”) started around 22:00, within the range of the participants’ habitual bedtime. The average sleep onset time when participants fell asleep in the scanner was 22:22 ( $SD = 25$  min). The average sleep latency was 8.16 ( $SD = 10.11$ ) min (Table 1). After the sleep session, participants were allowed to sleep in the nearby sleep laboratory for the remainder of the night.

## Tests of Cognitive Abilities

The Cambridge Brain Sciences (CBS) test battery was used to assess participants’ cognitive abilities, which has been used in large-scale studies (Wild, Nichols, Battista, Stojanoski, & Owen, 2018; Hampshire, Highfield, Parkin, & Owen, 2012). CBS is a Web-based battery of 12 cognitive tests that measures a broad range of cognitive abilities including reasoning, problem solving, planning, attention, and memory ([www.cambridgebrainsciences.com/tests](http://www.cambridgebrainsciences.com/tests)). A recent study, based on scores from a population-sized pool of 44,600 participants (Hampshire et al., 2012), revealed three factors that govern performance across the CBS subtests. These factors have been described as “Reasoning,” “STM,” and “Verbal” abilities (Hampshire et al., 2012).

The Reasoning factor is best described in terms of performance on five subtests adapted from the cognitive literature, including deductive reasoning (Cattell, 1949),

**Figure 1.** Experimental procedure. (a) Participants underwent initial screening to exclude any signs of sleep disorders, unusual sleep habits, or other health-related ineligibility and MRI compatibility requirements. (b) Eligible participants visited the sleep laboratory for the orientation session at least a week before the EEG–fMRI sleep recording night, in which participants were given detailed instructions about the study procedure, CBS tests, sleep diary, and an actiwatch. (c) All participants completed the CBS tests online and kept a regular sleep–wake cycle for at least 1 week before the sleep recording. Compliance

with this schedule was assessed using both sleep diaries and wrist actigraphy. (d) Participants who met these requirements were scheduled for the EEG–fMRI sleep recording session. The MRI scanning session started at 21:00, and lights out was from 22:00 to as late as 24:00.

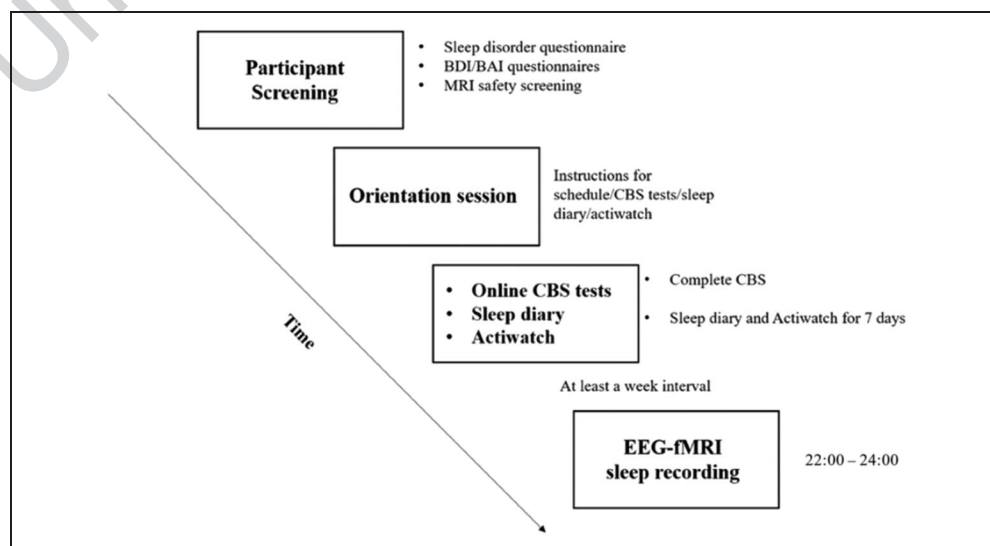


**Table 2.** Descriptive Statistics of the Three CBS Subscales (Reasoning, STM, and Verbal Abilities)

| <i>IQ Measures</i> | <i>Range</i> | <i>Mean (SD)</i> | <i>Median</i> |
|--------------------|--------------|------------------|---------------|
| Reasoning          | 78.84–108.17 | 95.65 (7.20)     | 96.46         |
| STM                | 84.38–115.33 | 101.60 (6.77)    | 102.30        |
| Verbal             | 88.51–110.92 | 99.62 (5.12)     | 99.52         |

spatial rotation (Silverman et al., 2000), feature match (Treisman & Gelade, 1980), spatial planning (Shallice, 1982), and interlocking polygons (Folstein, Folstein, & McHugh, 1975). STM is best described in terms of four subtests, including visuospatial working memory (Inoue & Matsuzawa, 2007), spatial span (Corsi, 1972), paired associates (Gould, Brown, Owen, Bullmore, & Howard, 2006), and self-ordered search (Collins, Roberts, Dias, Everitt, & Robbins, 1998). Finally, Verbal ability is best captured by performance on three subtests, including verbal reasoning (Baddeley, 1968), color–word remapping (Stroop, 1935), and digit span (Wechsler, 1981).

Consistent with the previous literature (Hampshire et al., 2012), the raw scores from each of the 12 subtests were normalized using the mean and standard deviation obtained from a large, young population ( $N = 44,600$ ; aged 20–35 years) of participants who completed the CBS battery (Hampshire et al., 2012). Each subtest was then weighted according to the factor loadings from Hampshire et al. (2012). Finally, the respective subtests were averaged to create the Reasoning, STM, and Verbal subscales and transformed to standard scores, so that scores were readily comparable with scores from similar studies that employed test batteries tapping into reasoning and verbal abilities, such as the Multidimensional Aptitude Battery–II (Fogel et al., 2007; Fogel & Smith, 2006), and other commonly used batteries of cognitive abilities (e.g., Wechsler Adult Intelligence Scale). The descriptive statistics of each subscale score are shown in Table 2.

### Polysomnographic Recording and Analysis

EEG was recorded using a 64-channel magnetic resonance (MR)-compatible EEG cap, which included one electrocardiogram (ECG) lead (Braincap MR, Easycap) and 64-channel EEG recorded via two MR-compatible 32-channel amplifiers (Brainamp MR Plus, Brain Products GmbH). EEG caps included scalp electrodes referenced to FCz. Using high-chloride abrasive electrode paste (Abralyt 2000 HiCL, Easycap), electrode skin impedance was reduced to  $< 5$  k $\Omega$ . To reduce movement-related EEG artifacts, participants' heads were immobilized in the MRI head coil using foam cushions. The EEG cap had a single drop-down ECG electrode, which has limited visualization of the r-peak of the QRS complex. For this reason, three

additional bipolar ECG recordings were taken using an MR-compatible 16-channel bipolar amplifier (Brainamp ExG MR, Brain Products GmbH) to obtain high-quality recordings and accurately visualize and identify r-peaks. As recommended by Mullinger, Yan, and Bowtell (2011), participants were positioned in the MRI scanner so that they were shifted away from the isocenter of the magnetic field by 40 mm. At this position, the quality of MRI images is not impacted, but the ballistocardiograph (BCG) artifact has been reported to be reduced by up to 40%, making BCG correction more straightforward. EEG was digitized at 5000 samples per second with a 500-nV resolution. Data were analog filtered by a band-limiter low-pass filter at 500 Hz and a high-pass filter with a 10-sec time constant corresponding to a high-pass frequency of 0.0159 Hz. Data were transferred via fiber-optic cable to a computer where Brain Products Recorder Software, Version 1.x was hardware synchronized to the scanner clock using the Brain Products “Sync Box” (Brain Products GmbH). The MRI sequence parameters were chosen so that the gradient artifact would be time stable, and the lowest harmonic of the gradient artifact (18.52 Hz) would occur above the spindle band (11–16 Hz). This was achieved by setting the MR scan repetition time to 2160 msec, such that it matched a common multiple of the EEG sample time (0.2 msec), the product of the scanner clock precision (0.1  $\mu$ sec), and the number of slices (40) used, as recommended in the literature (Mulert & Lemieux, 2009). EEG scanner artifacts were removed in two separate steps: (1) MRI gradient artifacts were removed using an adaptive average template subtraction method (Allen, Josephs, & Turner, 2000) implemented in Brain Products Analyzer and downsampled to 250 Hz, and (2) the r-peaks in the ECG were semiautomatically detected, visually verified, and manually adjusted when necessary, to correct both false-positive and false-negative r-peak detections. Then, adaptive template subtraction (Allen, Polizzi, Krakow, Fish, & Lemieux, 1998) was used to remove BCG artifacts time-locked to the r-peak of the cardiac rhythm QRS complex. After these steps, we visually verified the resulting quality of the data and inspected the amplitude of the residual artifacts time-locked to the r-peaks. An independent-component-analysis-based approach (Mantini et al., 2007; Srivastava, Crottaz-Herbette, Lau, Glover, & Menon 2005) was applied to remove any remaining BCG residual artifacts if the peak of the maximum amplitude of the residual artifact exceeded 3  $\mu$ V during the QRS complex (e.g., 0–600 msec). Finally, EEG was low-pass filtered (60 Hz) and rereferenced to the averaged mastoids.

After the artifact correction, sleep stages were scored in accordance with standard criteria (Iber et al., 2007) using the “VisEd Marks” toolbox ([https://github.com/jadesjardins/vised\\_marks](https://github.com/jadesjardins/vised_marks)) for EEGlab (Delorme & Makeig, 2004) during the wake resting state and sleep recording sessions. Automatic spindle detection was carried out using a previously published and validated (Ray et al., 2015) method employing EEGlab-compatible

(Delorme & Makeig, 2004) software (github.com/stuartfogel/detect\_spindles) written for MATLAB R2014a (The MathWorks Inc.). The detailed processing steps, procedures, and validation are extensively reported elsewhere (Ray et al., 2015) and are thus presented only briefly here. The spindle data were extracted from movement artifact-free, NREM sleep epochs. The detection method (Ray et al., 2015) used a complex demodulation transformation of the EEG signal with a bandwidth of 5 Hz centered about a carrier frequency of 13.5 Hz (i.e., 11–16 Hz; Iber et al., 2007). Spindle detection was visually verified by an expert scorer after automated detection. The variables of interest extracted from this method include spindle amplitude, duration, and density (number of spindles per minute of NREM sleep) for each participant. Results from full-bandwidth (11–16 Hz) spindles at Cz in NREM sleep were reported and included in the final analyses. Participants who had at least 30 spindle events were included in the fMRI analyses; however, all detected spindles were used for each of these participants. This approach is consistent with several previous EEG-fMRI studies that investigated brain activations time-locked to spindles (Fogel, Albouy, et al., 2017; Bergmann et al., 2012; Caporro et al., 2012; Andrade et al., 2011; Tyvaert et al., 2008; Laufs et al., 2007; Schabus et al., 2007).

## MRI Acquisition and Analysis

### *Recording Parameters*

Brain images were acquired using a 3.0-T Magnetom Prisma MRI system (Siemens) and a 64-channel head coil. In all participants, a structural T1-weighted MRI image was acquired using a 3-D magnetization prepared rapid gradient echo sequence (repetition time [TR] = 2300 msec, echo time = 2.98 msec, inversion time = 900 msec, flip angle = 9°, 176 slices, field of view = 256 × 256 mm<sup>2</sup>, matrix size = 256 × 256 × 176, voxel size = 1 × 1 × 1 mm<sup>3</sup>). Multislice T2\*-weighted fMRI images were acquired during the 8-min eyes-closed awake resting session and sleep session with a gradient echo-planar sequence using axial slice orientation (TR = 2160 msec, echo time = 30 msec, flip angle = 90°, 40 transverse slices, 3-mm slice thickness, 10% interslice gap, field of view = 220 × 220 mm<sup>2</sup>, matrix size = 64 × 64 × 40, voxel size = 3.44 × 3.44 × 3 mm<sup>3</sup>). Among all participants, up to 2.25 hr of sleep EEG-fMRI data was acquired.

### **Image Preprocessing**

Functional images were preprocessed and analyzed using SPM8 (www.fil.ion.ucl.ac.uk/spm/software/spm8/; Wellcome Department of Imaging Neuroscience) implemented in MATLAB (Ver. 8.5 R2015a) for Windows (Microsoft, Inc.). Functional scans of each session were realigned using rigid body transformations, iteratively optimized to minimize the residual sum of squares between

the first and each subsequent image separately for each session. A mean realigned image was then created from the resulting images. The structural T1 image was coregistered to this mean functional image using a rigid body transformation optimized to maximize the normalized mutual information between the two images. Coregistration parameters were then applied to the realigned BOLD time series. The coregistered structural images were segmented into gray matter, white matter, and cerebrospinal fluid. An average participant-based template was created using DARTEL in SPM8. All functional and anatomical images were spatially normalized using the resulting template, which was generated from the structural scans. Finally, spatial smoothing was applied on all functional images (Gaussian kernel, 8-mm FWHM).

### **PPI Analysis**

The PPI analysis refers to a method using a moderated multiple regression model to estimate task-dependent changes in the temporal association between a seed region and all voxels in the rest of the brain (McLaren, Ries, Xu, & Johnson, 2012). In the current study, two general linear models (GLMs) were generated for the PPI analyses, including a spindle-dependent activation GLM and a PPI GLM between the source regions and the brain activation time-locked to spindles, as described further in subsequent sections.

### *Sleep Spindle Event-related GLM*

For each participant, the first-level GLM was fit when considering brain responses time-locked to the onset of each spindle event. Consistent with previous studies (Bergmann et al., 2012; Andrade et al., 2011; Schabus et al., 2007), the event of interest vectors were composed of spindle onsets and were convolved with the canonical hemodynamic response function (HRF). Nuisance variables in the model included movement parameters estimated during realignment (translations in  $x$ ,  $y$ , and  $z$  directions and rotations around  $x$ ,  $y$ , and  $z$  axes), the squared value of the movement parameters, the first derivative of each movement parameter, and the square of the first derivative of each movement parameter as well as the mean white matter intensity and the mean cerebral spinal fluid intensity for each participant. Slow wave activity is a defining characteristic of NREM sleep (Iber et al., 2007) but is related to spindle generation (Siapas & Wilson, 1998). This activity was accounted for by including spectral power ( $\mu\text{V}^2$ ) in the delta band (0.5–4 Hz) for each TR window (2160 msec) as a variable of no interest, convolved with the HRF. Slow drifts were removed from the time series using a high-pass filter with a cutoff period of 128 sec. Serial correlations in the fMRI signal were estimated using an autoregressive (Order 1) plus white noise model and a restricted maximum likelihood algorithm.

### *PPI Analysis*

In the current study, the standard PPI model implemented in SPM8 was used. We aimed to investigate FC between the main regions recruited by spindles and other brain areas. Therefore, six independent ROIs were defined as source regions using WFU PickAtlas AAL template ([www.fmri.wfubmc.edu/software/PickAtlas](http://www.fmri.wfubmc.edu/software/PickAtlas)): (1) thalamus, (2) ACC, (3) bilateral putamen, (4) PCC, (5) medial PFC (mPFC), and (6) bilateral hippocampus. Specifically, ACC, thalamus, and bilateral putamen have been repeatedly reported to be recruited during spindle events (Fang et al., 2019; Fogel, Albouy, et al., 2017; Bergmann et al., 2012; Caporro et al., 2012; Andrade et al., 2011; Tyvaert et al., 2008; Laufs et al., 2007; Schabus et al., 2007). In addition, to investigate FC within the DMN, one of the most important networks to be explored during sleep (Koike, Kan, Misaki, & Miyauchi, 2011; Sämann et al., 2011; Horovitz et al., 2008, 2009; Larson-Prior et al., 2009), we also included the hub region of the DMN (i.e., the PCC) as an ROI in the current study. Although we did not observe mPFC and hippocampal activation time-locked to spindles in our previous study (Fang et al., 2019), these regions have been implicated as being recruited during spindle events. Specifically, EEG studies in rodents have observed neuronal activity in mPFC during spindle events (Peyrache, Battaglia, & Destexhe, 2011; Siapas & Wilson, 1998), and the mPFC is believed to be critical for general intelligence and reasoning-related tasks (Coricelli & Nagel, 2009; Gong et al., 2005; Gray et al., 2003; Waltz et al., 1999). In addition, according to previous EEG studies, hippocampal ripples have been shown to be time-locked to spindles, and temporal coupling between slow oscillations, spindles, and ripples has been suggested to support hippocampo-neocortical dialogue underlying memory consolidation during sleep (Clemens et al., 2007, 2011; Girardeau & Zugaro, 2011). Thus, the mPFC and bilateral hippocampus were also chosen as seed regions. After the procedure described by Andrade et al. (2011), task-related regressors (i.e., spindle events) were convolved with the HRF. The BOLD signal time course was extracted from the six ROIs (e.g., ACC, thalamus, bilateral putamen, PCC, mPFC, and hippocampus) and then was deconvolved using the HRF to get a neural representation of the presumed underlying neural activity. In PPI, the resulting regressor was forwarded to convolution with the binary vector of spindles. For each ROI, a model was set up comprising three regressors: (1) the psychological regressors (i.e., spindle regressors), (2) the physiological regressor of the BOLD signal time course of the six ROIs, and (3) their interaction terms. In the fixed effects model, these three regressors were convolved with the HRF to match the hemodynamically delayed fMRI responses. The interaction term was evaluated for each source region. Finally, the resulting first-level contrast was forwarded to the second-level GLM analyses using a one-sample *t* test. These GLM analyses generated statistical parametric

*t* maps [(SPM(T))] of PPI for each source region. The resulting maps were assessed at the threshold of uncorrected  $p < .001$ , cluster size  $> 50$  voxels at the whole-brain level, and statistically significant results reported for family wise error (FWE)-corrected values at  $p < .05$  at the cluster level (Hayasaka, Phan, Liberzon, Worsley, & Nichols, 2004).

Whole-brain multiple regression was used to investigate the relationship between the FC of each ROI and the cognitive abilities assessed by the CBS tests. PPI contrast maps of the *t* statistic [SPM(T)] from the first-level GLM were selected, and cognitive test scores for each subscale (i.e., Reasoning, Verbal, and STM) were included in the models as covariates of interest in separate second-level GLMs. Multiple regression analyses were conducted to explore which brain regions functionally connected with the source regions during spindle events and were also correlated to CBS subscale scores. Gender and whole-brain volume were included in the models as covariates of noninterest. These variables were included given that the relationship between spindles and reasoning ability differs in men and women (Ujma et al., 2014), and brain volume might influence NREM slow wave oscillations (Saletin, van der Helm, & Walker, 2013) or sleep quality (Branger et al., 2016) or be related to cognitive abilities (Casey, Tottenham, Liston, & Durston 2005). Again, the resulting maps were assessed at the threshold of uncorrected  $p < .001$ , cluster size  $> 50$  voxels at the whole-brain level, and statistically significant results reported for and FWE corrected values at  $p < .05$  at the cluster level (Hayasaka et al., 2004).

### *Awake Resting-state FC Analysis*

We examined further whether there was a similar relationship between waking FC and cognitive abilities. To assess the specificity of the spindle analyses, the same seed regions (i.e., ACC, thalamus, bilateral putamen, PCC, mPFC, bilateral hippocampus) were used for FC analysis on the 8-min-long session of awake resting-state data. Resting-state fMRI preprocessing and FC analyses were conducted using the Data Processing Assistant for Resting-State fMRI (Yan & Zang, 2010) plug-in for SPM8 using MATLAB (Ver. 8.5 R2015a). For image preprocessing, resting images of each participant were first realigned to correct for head motion, coregistered with the anatomical image, and spatially smoothed using a 3-D 4-mm FWHM Gaussian kernel. Images were then normalized to standard Montreal Neurological Institute space and resampled with an isotropic  $3 \times 3 \times 3$  mm<sup>3</sup> voxel size. Linear band-pass filtering at 0.01–0.08 Hz was used to reduce low-frequency drift and physiological high-frequency respiratory and cardiac noise. Nuisance covariates, including the Friston-24 head motion parameters (Friston, Williams, Howard, Frackowiak, & Turner, 1996), global mean signal, white matter signal, and cerebrospinal fluid signal, were regressed out of the data (Fair

et al., 2008). Next, for each participant, the mean BOLD fMRI signal time series were extracted from the seed regions and used as the regressor in the FC analysis. The correlation coefficients between the time series of each seed region and those of all other brain areas were transformed to  $z$  scores using Fisher's  $r$ -to- $z$  transformation. These  $z$ -transformed individual FC maps were then entered into the second-level whole-brain regression analysis to explore the relationship between the resting-state FC and cognitive abilities assessed by CBS. The threshold was set at the same threshold as PPI analyses of whole-brain-level uncorrected  $p < .001$ , cluster size  $> 50$  voxels, and cluster-level FWE-corrected  $p < .05$ .

## RESULTS

### Sleep Architecture

As shown in Table 1, among the 29 participants,  $N = 26$  participants experienced Stage 1 sleep (NREM1) because three participants fell asleep immediately (within 30 sec) upon the start of the EEG-fMRI session, all  $N = 29$  participants experienced NREM2 sleep,  $N = 20$  had slow wave sleep (SWS), and  $N = 8$  had rapid eye movement (REM) sleep. The ( $N = 29$ ) participants had more than 14.67 min of sleep and, on average, 44.20 ( $SD = 23.84$ ) min of sleep (including REM) during the sleep recording session in the MRI scanner. The average sleep latency of these 29 participants was 8.16 ( $SD = 10.11$ ) min, and the average sleep onset time when participants fell asleep in the scanner was 22:22 ( $SD = 25$ ) min. Given the focus of the current investigation on NREM spindles, only the NREM data of the 29 participants were analyzed. The average duration of NREM sleep was 39.29 ( $SD = 19.33$ )

min, and participants had, on average, 334.74 ( $SD = 212.29$ , min = 63, max = 1035) sleep spindles.

### FC Related to Sleep Spindles

First, seed-based PPI analysis was used to investigate FC during spindle events for the following regions: the thalamus and ACC, which are key regions of the thalamo-cortical circuitry; bilateral putamen from the BG network; the PCC; a hub of DMN; the mPFC; and the bilateral hippocampus. Figure 2 illustrates the FC map for all six ROIs during spindle events.

Figure 2A shows the FC map for ACC during spindle events, which was functionally connected to the thalamus, bilateral putamen, and bilateral anterior insula (aINS). As shown in Figure 2B, the thalamus was functionally connected to a widespread area of frontal cortex, from the anterior to the posterior areas, also including ACC, middle cingulate cortex (MCC), and PCC. Part of the cerebellum was also connected to the thalamus during spindle occurrences. As illustrated in Figure 2C, the bilateral putamen was largely connected to the motor cortical regions and the thalamus. Consistent with previous findings investigating FC across sleep stages (Koike et al., 2011; Sämann et al., 2011; Horovitz et al., 2008, 2009; Larson-Prior et al., 2009), clear DMN FC for PCC related to spindle events during NREM sleep was observed (Figure 2D), including the connectivity between the PCC and the bilateral parietal lobule, and with the mPFC. As another hub region of DMN, the mPFC was also functionally connected with the precuneus and PCC (Figure 2E), which is in line with the PCC-seed-based FC results. The bilateral hippocampus was mainly connected with surrounding parahippocampus and the

**Figure 2.** PPI interaction for Spindles  $\times$  Source Regions ( $p_{FWE}$ , cluster  $< 0.05$ , cluster size  $> 50$  voxels). FC maps for (A) ACC, (B) the thalamus, (C) the bilateral putamen, (D) the PCC, (E) the mPFC, and (F) the bilateral hippocampus.

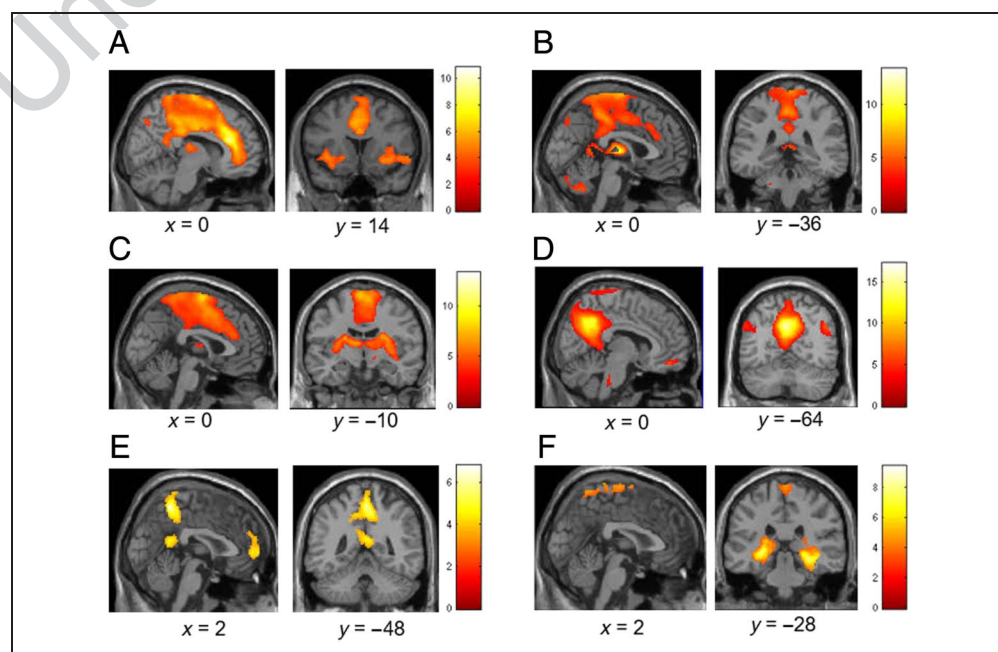
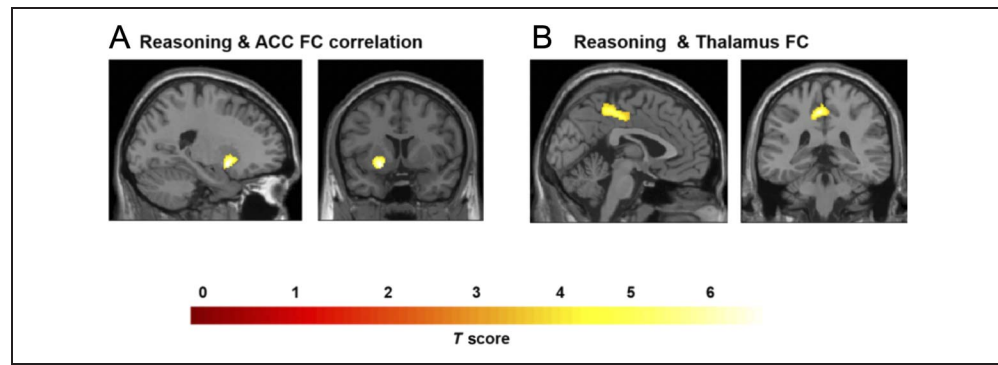


**Table 3.** FC during Sleep Spindles

| <i>Hemisphere</i>           | <i>Brain Region</i>  | <i>MNI Coordinate</i> |          |          | <i>Peak Voxel</i> | <i>p Value<br/>(Cluster-Level FWE)</i> |
|-----------------------------|----------------------|-----------------------|----------|----------|-------------------|--|
|                             |                      | <i>x</i>              | <i>y</i> | <i>z</i> | <i>t Value</i>    |  |
| <i>Thalamus FC</i>          |                      |                       |          |          |                   |  |
| Right                       | ACC                  | 4                     | 26       | 36       | 4.47              | <.05                                   |
| Left                        | Medial frontal gyrus | -2                    | -12      | 76       | 7.42              | <.001                                  |
| Left                        | MCC                  | 4                     | -32      | 48       | 5.21              | <.001                                  |
| Left                        | Cerebellum           | -40                   | -62      | -36      | 5.65              | .001                                   |
| Right                       | PCC                  | 2                     | -32      | 30       | 4.84              | <.001                                  |
| <i>ACC FC</i>               |                      |                       |          |          |                   |  |
| Left                        | Putamen              | -20                   | 6        | -10      | 6.6               | .009                                   |
| Right                       | Putamen              | 30                    | 12       | -8       | 5.34              | <.001                                  |
| Left                        | Insula               | -34                   | 18       | -8       | 5.17              | .009                                   |
| Right                       | Insula               | 36                    | 14       | -6       | 4.35              | <.001                                  |
| Right                       | Thalamus             | 10                    | -20      | 12       | 4.94              | .011                                   |
| <i>Bilateral Putamen FC</i> |                      |                       |          |          |                   |  |
| Left                        | MCC                  | -8                    | 4        | 50       | 7.67              | <.001                                  |
| Right                       | ACC                  | 2                     | 32       | 26       | 5.24              | <.001                                  |
| Right                       | Medial frontal gyrus | 2                     | 0        | 56       | 6.72              | <.001                                  |
| Left                        | Thalamus             | -10                   | -8       | 10       | 7.03              | <.001                                  |
| <i>PCC FC</i>               |                      |                       |          |          |                   |  |
| Left                        | Parietal lobule      | -50                   | -72      | 32       | 8.42              | .001                                   |
| Right                       | Parietal lobule      | 48                    | -64      | 32       | 6.76              | .003                                   |
| Right                       | Medial frontal gyrus | 8                     | 48       | -14      | 6.21              | <.05                                   |
| <i>mPFC FC</i>              |                      |                       |          |          |                   |  |
| Right                       | Precuneus            | 2                     | -48      | 56       | 6.83              | <.001                                  |
| Right                       | PCC                  | 4                     | -50      | 16       | 4.83              | .015                                   |
| Left                        | PCC                  | -4                    | -48      | 24       | 4.22              | .015                                   |
| <i>Hippocampus FC</i>       |                      |                       |          |          |                   |  |
| Right                       | SMA                  | 4                     | -8       | 76       | 4.98              | <.001                                  |
| Right                       | Parahippocampus      | 28                    | -24      | -14      | 9.43              | <.001                                  |
| Left                        | Parahippocampus      | -26                   | -22      | -16      | 7.38              | <.001                                  |

Significant brain responses after FWE correction  $p < .05$  at the cluster level, with cluster size  $> 50$  voxels.

**Figure 3.** (A) Correlation between Spindles × ACC interaction and Reasoning ability ( $p_{FWE}$ , cluster < 0.05, cluster size > 50 voxels). (B) Correlation between Spindles × Thalamus interaction and Reasoning ability ( $p_{FWE}$ , cluster < 0.05 correction threshold, cluster size > 50 voxels).



SMA (Figure 2F). Detailed statistical significance of the whole-brain results is reported in Table 3.

### Correlation between Spindle-related FC and Cognitive Abilities

To examine the relationship between spindle-specific FC and cognitive abilities, whole-brain spatial correlation analyses were conducted between the FC map of the six source regions and the scores of the three cognitive factors (i.e., Reasoning, STM, and Verbal abilities) assessed by the CBS tests. Among the six source regions, reasoning ability was significantly correlated with spindle-specific FC for ACC and thalamus, including the FC between ACC and the left putamen (see Figure 3A;  $[-22, 8, -10]$ ,  $t = 5.7$ ,  $p_{FWE, cluster} < 0.05$ , cluster size > 50 voxels), and the FC between the thalamus and the MCC (see Figure 3B;  $[-6, -36, 48]$ ,  $t = 4.6$ ,  $p_{FWE, cluster} < 0.05$ , cluster size > 50 voxels). No such correlation was found between cognitive abilities and FC for the other source regions. Consistent with previous EEG-only studies, no spindle-related connectivity was correlated with STM or Verbal abilities. These results suggest that the magnitude of spindle-related FC between ACC and the left putamen and between the thalamus and the MCC is

specifically correlated with Reasoning, but not STM or Verbal abilities.

To assess the effect size, we conducted ROI analyses to extract the FC values between ACC and the left putamen, and furthermore, between the thalamus and the MCC, and performed standard regression analyses using SPSS 24.0 (IBM). After controlling for gender and whole-brain volume, we found the same relationship as shown in the whole-brain results, that is, that ACC–left putamen FC and thalamus–MCC FC were significantly correlated with reasoning ability (Table 4). Using Cohen’s  $f^2$  (Selya, Rose, Dierker, Hedeker, & Mermelstein, 2012; Cohen, 1988), we calculated the effect size of the regression effects of spindle-related FC on reasoning ability. As shown in Table 4, the effect size for ACC–left putamen FC is  $f^2 = 1.32$ , and the effect size for thalamus–MCC FC is  $f^2 = 0.61$ , which are considered large effect sizes (Selya et al., 2012; Cohen, 1988). The partial correlation scatterplots between spindle-related FC and reasoning ability are shown in Figure 4.

### Awake Resting-state FC

As shown in Figure 5, compared with the FC related to spindles, the overall FC is more robust during the awake

**Table 4.** Regression Analysis and Effect Size for the Relationship between Spindle-Related FC and Reasoning Ability

| <i>Regression Effects for ROIs</i>           |                                       |            |             |               |
|--|---------------------------------------|------------|-------------|---------------|
|  | $R^2$                                 | $F(3, 25)$ | $p$ Value   | Cohen’s $f^2$ |
| ACC–L.putamen FC                             | .598                                  | 12.41      | <.001       | 1.32          |
| Thalamus–MCC FC                              | .421                                  | 6.05       | .003        | 0.61          |
| <i>Partial Correlation Post Hoc Analyses</i> |                                       |            |             |               |
|  | Standardized Coefficients ( $\beta$ ) | $t$ Value  | Partial $r$ | $p$ Value     |
| ACC–L.putamen FC                             | 0.737                                 | 5.755      | 0.755       | <.001         |
| Thalamus–MCC FC                              | 0.613                                 | 3.913      | 0.616       | .001          |

L = left.

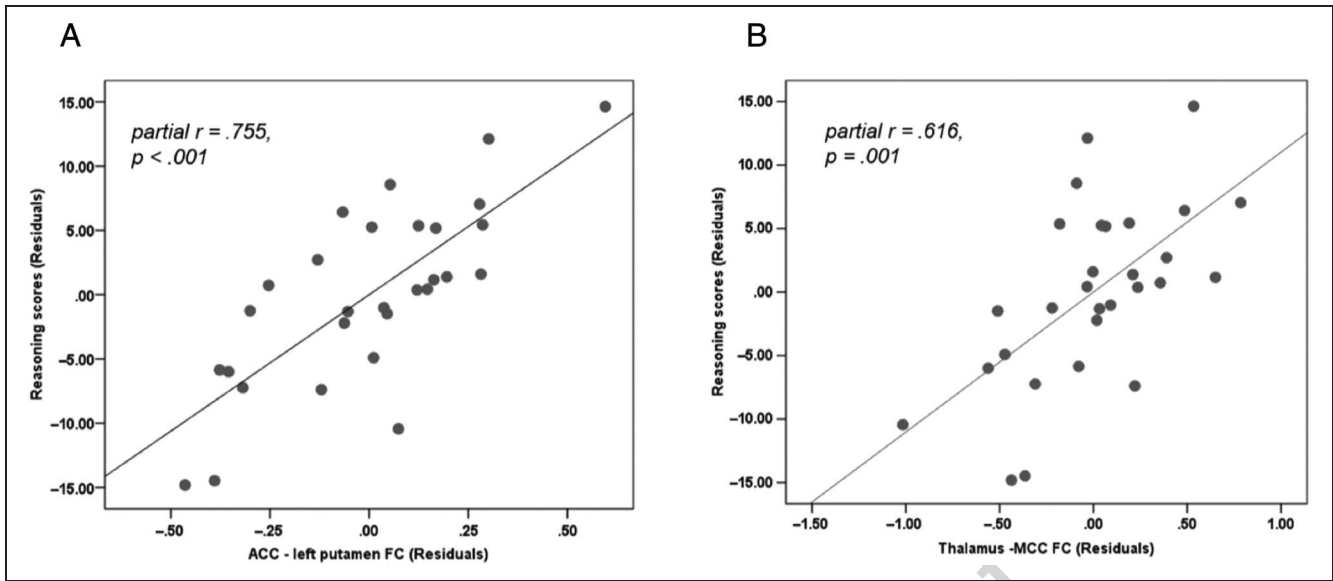


**Figure 4.** Semipartial correlation between spindle-related FC and reasoning ability. (A) Correlation between ACC-left putamen FC and reasoning ability (partial  $r = .755$ ,  $p < .001$ ). (B) Correlation between thalamus-MCC FC and reasoning ability (partial  $r = .616$ ,  $p = .001$ ).

resting state, especially connectivity in cerebellum and BG regions. Notably, the FC pattern in key regions during wake is similar to the FC results related to spindles, particularly in the thalamo-cortical-BG network and the DMN. Detailed statistical significance information for the whole-brain results is shown in Table 5. These results are consistent with the findings of previous studies indicating that the brain network patterns during sleep are similar to those during wakefulness (Houldin, Fang, Ray, Owen, & Fogel, 2019; Horowitz et al., 2009; Larson-Prior et al., 2009).

We also conducted regression analyses to investigate the relationship between FC during wakefulness and

cognitive abilities. However, there was no significant correlation between FC and reasoning, STM, or verbal abilities. These findings suggest that the extent of inter-individual differences in FC in the thalamus, cortical, and striatal regions was significantly related to reasoning abilities only during sleep spindles, but not during wakefulness.

## DISCUSSION

In the current study, the functional significance of the extent of interindividual differences in FC between known hub regions activated during spindle events (including

**Figure 5.** FC during awake resting state ( $p_{FWE}$ , cluster  $< 0.05$ , cluster size  $> 50$  voxels). FC maps for (A) ACC, (B) the thalamus, (C) the bilateral putamen, (D) the PCC, (E) the mPFC, and (F) the bilateral hippocampus.

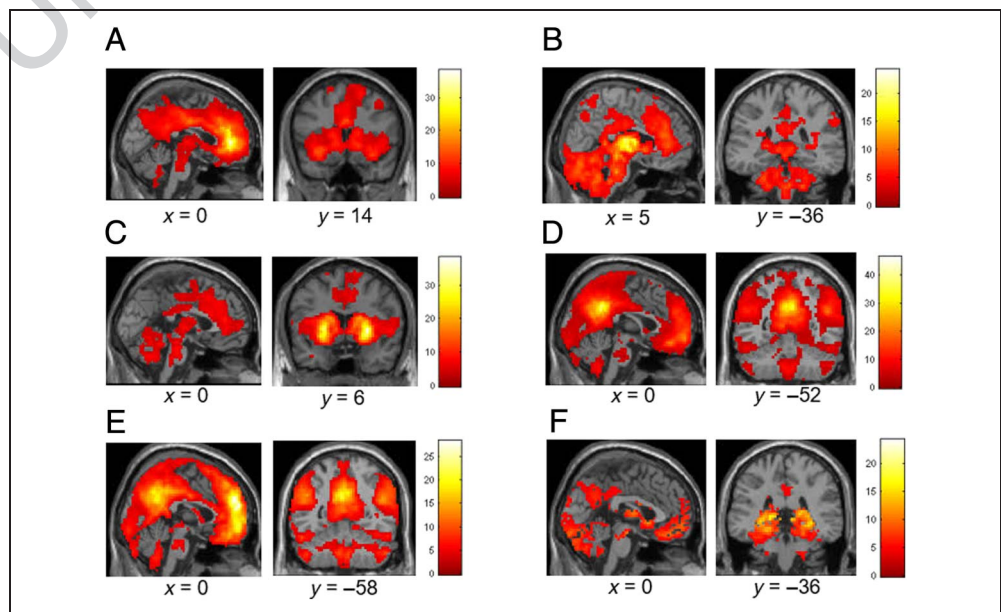


**Table 5.** Awake Resting-State FC

| <i>Hemisphere</i>           | <i>Brain Region</i>      | <i>MNI Coordinate</i> |          |          | <i>Peak Voxel</i> | <i>p Value<br/>(Cluster-Level FWE)</i> |
|-----------------------------|--------------------------|-----------------------|----------|----------|-------------------|--|
|                             |                          | <i>x</i>              | <i>y</i> | <i>z</i> | <i>t Value</i>    |  |
| <i>ACC FC</i>               |                          |                       |          |          |                   |  |
| Left                        | Caudate                  | -12                   | 12       | 6        | 10.74             | <.001                                  |
| Right                       | Caudate                  | 15                    | 15       | -3       | 11.41             | <.001                                  |
| Left                        | Putamen                  | -15                   | 6        | -3       | 8.60              | <.001                                  |
| Right                       | Putamen                  | 21                    | 6        | -6       | 10.02             | <.001                                  |
| Left                        | Insula                   | -33                   | 18       | -12      | 13.32             | <.001                                  |
| Right                       | Insula                   | 30                    | 18       | -12      | 15.23             | <.001                                  |
| Middle                      | MCC                      | 0                     | -12      | 33       | 16.55             | <.001                                  |
| Left                        | Thalamus                 | -6                    | -12      | 0        | 8.28              | <.001                                  |
| Right                       | Thalamus                 | 6                     | -12      | 3        | 10.78             | <.001                                  |
| Left                        | Precuneus                | -9                    | -60      | 27       | 11.47             | <.001                                  |
| Right                       | Precuneus                | 12                    | -57      | 36       | 10.78             | <.001                                  |
| Left                        | PCC                      | -9                    | -45      | 27       | 10.93             | <.001                                  |
| Right                       | PCC                      | 9                     | -45      | 27       | 9.12              | <.001                                  |
| Left                        | Inferior parietal cortex | -48                   | -60      | 51       | 6.80              | <.001                                  |
| Right                       | Inferior parietal cortex | 57                    | -48      | 45       | 6.50              | <.001                                  |
| Left                        | Cerebellum               | -45                   | -45      | -42      | 6.47              | <.001                                  |
| Right                       | Cerebellum               | 30                    | -42      | -33      | 6.33              | <.001                                  |
| <i>Thalamus FC</i>          |                          |                       |          |          |                   |  |
| Right                       | ACC                      | -6                    | 36       | 15       | 11.29             | <.001                                  |
| Left                        | MCC                      | 3                     | -18      | 42       | 5.91              | <.001                                  |
| Right                       | SMA                      | 3                     | 18       | 48       | 6.70              | <.001                                  |
| Left                        | PCC                      | -3                    | -39      | 27       | 6.11              | <.001                                  |
| Right                       | PCC                      | 6                     | -36      | 27       | 5.98              | <.001                                  |
| Left                        | Caudate                  | -18                   | 18       | 9        | 12.54             | <.001                                  |
| Right                       | Caudate                  | 12                    | 18       | 3        | 9.20              | <.001                                  |
| Left                        | Putamen                  | -30                   | -6       | -6       | 8.96              | <.001                                  |
| Right                       | Putamen                  | 24                    | 3        | -6       | 8.54              | <.001                                  |
| Left                        | Cerebellum               | -12                   | -51      | -39      | 13.30             | <.001                                  |
| Right                       | Cerebellum               | 15                    | -48      | -39      | 12.54             | <.001                                  |
| Left                        | Pons                     | -3                    | -24      | -33      | 11.44             | <.001                                  |
| <i>Bilateral Putamen FC</i> |                          |                       |          |          |                   |  |
| Left                        | ACC                      | -6                    | 27       | 24       | 10.30             | <.001                                  |
| Right                       | ACC                      | 6                     | 39       | 15       | 11.36             | <.001                                  |
| Left                        | MCC                      | -6                    | 18       | 36       | 9.15              | <.001                                  |
| Right                       | MCC                      | 9                     | 18       | 36       | 10.12             | <.001                                  |

**Table 5.** (continued)

| <i>Hemisphere</i>               | <i>Brain Region</i>           | <i>MNI Coordinate</i> |          |          | <i>Peak Voxel</i> | <i>p Value<br/>(Cluster-Level FWE)</i> |
|---------------------------------|-------------------------------|-----------------------|----------|----------|-------------------|--|
|                                 |                               | <i>x</i>              | <i>y</i> | <i>z</i> | <i>t Value</i>    |  |
| Middle                          | Superior medial frontal gyrus | 0                     | 30       | 36       | 7.58              | <.001                                  |
| Left                            | Thalamus                      | 6                     | -12      | 3        | 12.11             | <.001                                  |
| Left                            | Cerebellum                    | -33                   | -37      | -27      | 6.41              | <.001                                  |
| Right                           | Cerebellum                    | 18                    | -75      | -27      | 5.69              | <.001                                  |
| <i>PCC FC</i>                   |                               |                       |          |          |                   |  |
| Right                           | Medial OFC                    | 3                     | 60       | -9       | 22.93             | <.001                                  |
| Right                           | Superior medial frontal gyrus | 6                     | 60       | 18       | 15.87             | <.001                                  |
| Left                            | Superior medial frontal gyrus | -3                    | 66       | 12       | 14.44             | <.001                                  |
| Left                            | Middle frontal cortex         | -39                   | 21       | 45       | 12.58             | <.001                                  |
| Left                            | Parietal lobule               | -42                   | -72      | 42       | 19.67             | <.001                                  |
| Right                           | Parietal lobule               | 45                    | -57      | 30       | 19.93             | <.001                                  |
| Left                            | Middle temporal lobe          | -45                   | 15       | -30      | 9.97              | <.001                                  |
| Right                           | Middle temporal lobe          | 66                    | -15      | -15      | 17.33             | <.001                                  |
| Middle                          | Pons                          | 0                     | -24      | -39      | 5.89              | <.001                                  |
| Left                            | Cerebellum                    | -21                   | -87      | -21      | 7.73              | <.001                                  |
| Right                           | Cerebellum                    | 21                    | -84      | -18      | 8.16              | <.001                                  |
| <i>Medial Frontal Cortex FC</i> |                               |                       |          |          |                   |  |
| Left                            | PCC                           | -3                    | -54      | 30       | 21.03             | <.001                                  |
| Left                            | Precuneus                     | -3                    | -57      | 9        | 12.72             | <.001                                  |
| Right                           | Precuneus                     | 5                     | -54      | 33       | 18.96             | <.001                                  |
| Left                            | MCC                           | -3                    | -45      | 36       | 17.90             | <.001                                  |
| Left                            | Middle frontal cortex         | -45                   | 18       | 42       | 14.25             | <.001                                  |
| Right                           | Middle frontal cortex         | 42                    | 15       | 48       | 13.17             | <.001                                  |
| Left                            | Parietal lobule               | -48                   | -63      | 33       | 18.80             | <.001                                  |
| Right                           | Parietal lobule               | 54                    | -63      | 36       | 16.52             | <.001                                  |
| Left                            | Caudate                       | -12                   | 12       | 12       | 9.81              | <.001                                  |
| Right                           | Caudate                       | 12                    | 15       | 9        | 11.40             | <.001                                  |
| Left                            | Insula                        | -27                   | 12       | -18      | 11.07             | <.001                                  |
| Right                           | Insula                        | 30                    | 21       | -18      | 8.51              | <.001                                  |
| Left                            | Midbrain                      | -3                    | -24      | -6       | 5.72              | <.001                                  |
| Left                            | Pons                          | -3                    | -24      | -24      | 6.40              | <.001                                  |
| Left                            | Cerebellum                    | -33                   | -78      | -36      | 10.03             | <.001                                  |
| Right                           | Cerebellum                    | 27                    | -81      | -36      | 12.63             | <.001                                  |

**Table 5.** (continued)

| Hemisphere            | Brain Region    | MNI Coordinate |          |          | Peak Voxel     | <i>p</i> Value<br>(Cluster-Level FWE) |
|-----------------------|-----------------|----------------|----------|----------|----------------|---------------------------------------|
|                       |                 | <i>x</i>       | <i>y</i> | <i>z</i> | <i>t</i> Value |                                       |
| <i>Hippocampus FC</i> |                 |                |          |          |                |                                       |
| Right                 | Medial OFC      | 3              | 51       | -12      | 8.69           | <.001                                 |
| Left                  | Precuneus       | -12            | -42      | 6        | 12.67          | <.001                                 |
| Right                 | Precuneus       | 12             | -45      | 6        | 8.08           | <.001                                 |
| Middle                | PCC             | 0              | -57      | 30       | 5.92           | <.001                                 |
| Left                  | Parahippocampus | -27            | -36      | -9       | 9.81           | <.001                                 |
| Right                 | Parahippocampus | 26             | -36      | -10      | 11.54          | <.001                                 |
| Left                  | Temporal pole   | -45            | 12       | -33      | 8.49           | <.001                                 |
| Right                 | Temporal pole   | 45             | 18       | -33      | 6.65           | <.001                                 |
| Right                 | Thalamus        | 3              | -6       | 9        | 9.93           | <.001                                 |
| Middle                | Midbrain        | 0              | -24      | -21      | 6.19           | .013                                  |
| Left                  | Cerebellum      | -21            | -87      | -27      | 8.24           | <.001                                 |
| Right                 | Cerebellum      | 9              | -84      | -33      | 10.33          | <.001                                 |

Significant brain responses after FWE correction  $p < .05$  at the cluster level, with cluster size  $> 50$  voxels.

the thalamus, ACC, bilateral putamen, PCC, mPFC, and hippocampus) and the rest of the brain was explored. Specifically, we investigated whether spindle-dependent FC was related to interindividual differences in Reasoning, STM, and Verbal intellectual abilities. Sleep spindles during NREM sleep were found to induce brain connectivity within the thalamo-cortical-BG network and the DMN. Interestingly, during spindle events, the extent of FC between ACC and the left putamen, and between the thalamus and the MCC, was exclusively related to reasoning, but not verbal or STM abilities. These results suggest that, during spontaneous spindle events, the extent of communication between brain regions involved in spindle generation and other brain regions, such as the putamen and cingulate cortex, is related to our ability to identify complex patterns and relationships and the use of logic, skills, and ability to solve novel problems (i.e., related to individual differences in “fluid intelligence”).

### Thalamo-cortical–BG Connectivity Interacts with Spindles

Connectivity between thalamic and cortical regions was observed during sleep spindle events in NREM sleep, specifically in ACC, MCC, PCC, and part of the cerebellum. Prior EEG studies have shown that spindles are generated from rhythmic and synchronized communication in the thalamocortical–reticular circuit and terminated by desynchronization of thalamic and cortical neuronal firing (Bonjean et al., 2011; Steriade, Nuñez, & Amzica, 1993; von Krosigk, Bal, & McCormick, 1993; Purpura, 1968). Previous EEG-fMRI studies have also reported

brain activations in the thalamus and cortical regions time-locked to spindles but have not looked into the FC between these two hubs during spindle events (Caporro et al., 2012; Tyvaert et al., 2008; Laufs et al., 2007; Schabus et al., 2007) or the functional significance of these activations. Furthermore, electrophysiological and neuroimaging studies have clearly demonstrated the importance of thalamo-cortical networks in sleep (see Bagshaw & Khalsa, 2013, for a review). Specifically, previous studies have observed thalamo-cortical FC decreases in NREM1 followed by increases in NREM2 and SWS, which has been attributed to the presence of spindles (Tagliazucchi & Laufs, 2014; Picchioni, Duyn, & Horovitz, 2013; Spoormaker et al., 2010). The present results are consistent with these findings, and specifically link thalamo-cortical functional coupling to sleep spindles, at the whole-brain systems level.

In addition to the thalamus and PFC, the bilateral putamen has also been shown to be recruited during sleep spindles (Fang et al., 2019; Caporro et al., 2012; Tyvaert et al., 2008). Here, these regions (e.g., putamen, PFC) were functionally connected with the thalamus and cortical regions during sleep spindles. BG-thalamo-cortical circuits have been found to subserve motor, oculomotor, and other cognitive functioning such as learning and sleep-dependent memory consolidation in prior studies (Doyon et al., 2009; Doyon & Benali, 2005; Doyon & Ungerleider, 2002; Brown & Marsden, 1998). Furthermore, in this study, parts of the cerebellum were found to be functionally connected with the thalamus during spindles, which is in line with previous studies indicating that the cerebellum is recruited during spindle events

(Fang et al., 2019; Schabus et al., 2007), although this region is often overlooked in cognitive neuroimaging studies. Taken together, our findings suggest that, during spindle events, brain activity in the thalamus, cortical regions, and BG are temporally synchronized, indicating that these spatially separated regions are functionally connected to one another. These results also corroborate findings that spindles may be intimately involved in motor procedural memory consolidation (Fogel, Albouy, et al., 2017; Fogel, Vien, et al., 2017; Fogel et al., 2014; Doyon et al., 2009; Morin et al., 2008). Support for this idea comes from recent findings from our group, showing that the putamen is a hub for memory-consolidation-related FC during NREM sleep (Vahdat, Fogel, Benali, & Doyon, 2017) and is reactivated during spindle events after motor learning (Fogel, Albouy, et al., 2017).

### **DMN Connectivity Related to Spindles**

Our study revealed for the first time that the bilateral inferior parietal lobule and the mPFC were functionally connected with the PCC seed during spindle events, which make up the classic DMN. Using mPFC as a seed region, we also observed connectivity between the mPFC and both the precuneus and the PCC, which further supports the notion that the DMN is preserved as a functionally active region during NREM sleep. Recent studies investigating DMN connectivity during sleep have revealed that DMN connectivity persists during light sleep (i.e., NREM1; Koike et al., 2011; Sämann et al., 2011; Horovitz et al., 2008, 2009; Larson-Prior et al., 2009), whereas during deep sleep (i.e., NREM3), FC between nodes of the DMN is reduced (Horovitz et al., 2009). More specifically, the correlations of the posterior part of the DMN (e.g., PCC and inferior parietal lobule connections) hold strong, while the frontal areas (i.e., ACC, mPFC) are isolated from posterior DMN (Koike et al., 2011; Sämann et al., 2011; Horovitz et al., 2008, 2009; Larson-Prior et al., 2009). Studies of FC performed under anesthesia (Boveroux et al., 2010) and in disorders of consciousness (Vanhaudenhuyse et al., 2010) have suggested that DMN integrity is a neural correlate of consciousness (see Tagliazucchi & van Someren, 2017, for a review). Specifically, the uncoupling of posterior and anterior DMN nodes has been reported during states of reduced consciousness such as epilepsy (Blumenfeld, 2005), anesthesia (MacDonald, Naci, MacDonald, & Owen, 2015), disorders of consciousness (Laureys, 2005), and deep sleep (Horovitz et al., 2009). These studies examined DMN connectivity across sleep stages, whereas our study further illustrates the association between integrated DMN connectivity and, importantly, sleep spindles specifically. These results are consistent with spindles serving a sleep-protective role by shielding the brain from external stimuli (Schabus et al., 2012; Dang-Vu, McKinney, Buxton, Solet, & Ellenbogen, 2010; Vyazovskiy, Achermann, Borbély, & Tobler, 2004; Cote,

Epps, & Campbell, 2000; Elton et al., 1997; Peters & Jones, 1991), thereby enhancing a more internally focused state of consciousness reflected by enhanced DMN FC.

### **Saliency Network Connectivity Related to Spindles**

FC between ACC and bilateral aINS was also observed, regions that are part of the salience network (Picchioni et al., 2014; Yuan et al., 2012). This is consistent with previous findings demonstrating that the insula is related to the electrophysiological events of sleep, including slow waves (Murphy et al., 2009; Braun et al., 1997), spindles (Andrade et al., 2011; Schabus et al., 2007), and K-complexes (Caporro et al., 2012). A recent animal study has found that the aINS plays an important role in the regulation of sleep and motor behavior rhythmicity across multiple time scales (Chen et al., 2016). Using a seed-based FC approach, Martuzzi, Ramani, Qiu, Rajeevan, and Constable (2010) observed increased connectivity between insula and left ACC during SWS (see Heine et al., 2012, for a review), which is also consistent with our findings. Taken together, the results suggest that spindle events might contribute to communication within the salience network during NREM sleep.

### **Hippocampal FC Related to Spindles**

The bilateral hippocampus was found to be functionally connected with surrounding parahippocampus and SMA in the current study. Reactivation of hippocampus time-locked with sleep spindles has been observed after motor sequence learning (MSL; Fogel, Albouy, et al., 2017; Albouy, King, Maquet, & Doyon, 2013) and declarative learning (Jegou et al., 2019; Bergmann et al., 2012). Furthermore, the SMA has been reported to be involved in MSL (Lehéricy et al., 2004, 2005) and to be recruited during fast spindle events (Andrillon et al., 2011; Schabus et al., 2007). Although FC between bilateral hippocampus and SMA might be related to memory consolidation during sleep spindles (as has been found in prior studies, although this was not examined specifically in this study), here, we did not observe any relationship between FC in these regions and intellectual abilities. In addition, it is also worth noting that previous EEG studies have revealed that the incidence of hippocampal ripples is temporally related to the occurrence of spindles. Temporal coupling between slow oscillations, spindles, and ripples has been suggested to support a hippocampal–neocortical dialogue underlying memory consolidation (Clemens et al., 2007, 2011; Girardeau & Zugaro, 2011). Indeed, hippocampal FC related to spindles has been observed postlearning on memory tasks that are hippocampal dependent and related to spindles. For example, using coherence-based metrics on EEG data within the spindle band, Boutin et al. (2018) observed connectivity between hippocampus and motor cortex, putamen, and thalamus on the night

after MSL, but no such connectivity was found on a control night. Similar findings were reported in an animal EEG study (Benchenane et al., 2010) and a human EEG-fMRI study (Herweg et al., 2016). In the current study, there was no presleep hippocampal-dependent memory task performed; therefore, it is not surprising that we did not find the hippocampus to be functionally connected with additional ROIs during spindle events.

### **Spindle-related FC Correlated with Cognitive Abilities**

In addition to exploring FC related to sleep spindles, the main aim of the current study was to investigate the significance of this FC to human intelligence (i.e., cognitive abilities assessed by the CBS test battery). It is well established that sleep spindles are highly correlated with inter-individual differences in intellectual abilities, especially reasoning ability, that is, the capacity for problem solving (Fang et al., 2017; Ujma et al., 2014, 2015; Bódizs et al., 2005, 2008; Fogel et al., 2007; Schabus et al., 2006; Nader & Smith, 2001, 2003). Our previous work demonstrated that a subset of brain regions whose activation was time-locked to spindles was associated with reasoning ability, but not STM or verbal abilities (Fang et al., 2019). Here, we show, for the first time, that the extent of connectivity in this network of brain areas, as driven by sleep spindles, is related to human cognitive abilities. Consistent with previous EEG and cognitive studies (Fang et al., 2017, 2019; Fogel et al., 2007), spindle-related FC (between ACC–putamen and between thalamus–PCC) was uniquely correlated with reasoning but not STM or verbal abilities.

As key nodes in the cortical–striatal circuit, both the prefrontal region and putamen have been reported to be recruited in reasoning-related performance. For example, the level of functional activation and gray matter intensity of mPFC have been found to be positively correlated with general intelligence and reasoning-related tasks (Coricelli & Nagel, 2009; Gong et al., 2005; Gray et al., 2003; Waltz et al., 1999). In addition, the putamen is more active during reasoning-related tasks compared with other cognitive tasks (Rodríguez-Moreno & Hirsch, 2009; Melrose et al., 2007). Although no studies have directly examined the relationship between ACC–putamen FC and reasoning ability, previous research has revealed that dopamine function throughout the frontal–striatal circuit influences cognitively complex category learning performance, such as in the information integration task (Price, 2005) and Wisconsin Card Sorting Test (Rybakowski et al., 2005; Weinberger, Berman, Suddath, & Torrey, 1992). In addition, previous studies have found that connectivity between putamen and frontal regions, especially the rostral ACC region, is linked to higher-order cognitive performance, including executive control (Di Martino et al., 2008), conflict monitoring, and error-related processes (Kouneiher, Charron, & Koechlin, 2009; Carter & van Veen, 2007; Botvinick, Cohen, &

Carter, 2004; Ullsperger & von Cramon, 2004). These cognitive functions are required for reasoning-related information processing. Taken together with the results of the current study, this suggests that ACC and putamen are not only activated as separate regions during spindle events but also are functionally connected with each other as a network during spindle events. The extent of communication between ACC and the putamen was specifically correlated with the interindividual differences in reasoning ability over and above both verbal and STM abilities, which suggests that functional coupling between ACC and the putamen during spindle events supports cognitive functions that are related to “fluid intelligence,” but not “crystallized intelligence.”

In addition, reasoning abilities were correlated with FC between the thalamus and the MCC, areas that are a part of the thalamo-cortical circuitry. A number of studies have demonstrated that both the thalamus (Bohlken et al., 2014; Liang, Jia, Taatgen, Zhong, & Li, 2014; Jia et al., 2011; Melrose et al., 2007) and PFC (Coricelli & Nagel, 2009; Gong et al., 2005; Gray et al., 2003; Duncan, 2000; Waltz et al., 1999; Baker et al., 1996) are functionally engaged while performing reasoning tasks. Interestingly, previous research has suggested that deficient gating mechanisms of thalamo-cortical circuitry may account for abnormal spindle generation in children with intellectual disability (Shibagaki & Kiyono, 1983; Bixler & Rhodes, 1968; Gibbs & Gibbs, 1962). Moreover, reduced FC between thalamus and PFC in patients with schizophrenia is associated with deficits in attention, executive functioning, and processing speed (for a review, see Sheffield & Barch, 2016).

Our results suggest that stronger spindle-dependent communication within these networks of brain regions is associated with greater reasoning abilities. Thus, the efficient functioning of the neural substrates that support spindle generation and communication among regions that are recruited during spontaneous spindle events may be related to intellectual ability. Spindles emanate from highly synchronized oscillatory communication between widespread connections between the thalamus and the neocortex. Greater spindle-related functional communication within this extended thalamocortical network could have implications for intellectual abilities and the maintenance of knowledge. Thus, normal and efficient generation of spindles may support normal intellectual abilities. For example, highly efficient generation of spindles may support more highly developed cognitive aptitudes, as suggested by a strong correlation between spindles and IQ in individuals in the gifted range (Fogel et al., 2007). By contrast, deficient or dysfunctional spindle generation may be associated with compromised intellectual functioning (Gibbs & Gibbs, 1962).

Furthermore, the patterns of FC during sleep spindles were found to be similar to awake resting-state FC. This is consistent with previous findings that show the overall spatio-temporal patterns of resting-state brain networks

(RSNs) during sleep are similar to RSNs observed during wakefulness (Horowitz et al., 2009; Larson-Prior et al., 2009) and that no unique sleep-specific RSNs have been identified (Houldin et al., 2019). Importantly, here, we show that there was no similar significant relationship between the extent of waking FC and intellectual abilities. These results provide additional support that, despite the existence of outwardly similar functional networks of brain regions during both wake and sleep, the extent of FC occurring during spindle events appears to be specifically related to reasoning abilities.

However, there are several limitations to this study worth mentioning. An important limitation is that these data are entirely correlational. Thus, the directionality of these effects cannot be determined, and other confounding or unrelated factors might partly explain the observed correlations between the spindle-related FC and reasoning ability. However, our previous research has demonstrated that other factors that relate to spindles, such as sleep maintenance (Schabus et al., 2012; Dang-Vu et al., 2010; Vyazovskiy et al., 2004; Cote et al., 2000; Elton et al., 1997; Peters & Jones, 1991) and chronobiological rhythms (Cajochen, Münch, Knoblauch, Blatter, & Wirz-Justice, 2006; Knoblauch et al., 2005; Knoblauch, Martens, Wirz-Justice, Kräuchi, & Cajochen, 2003; Dijk & Cajochen, 1997; Dijk & Czeisler, 1995; Dijk, Hayes, & Czeisler, 1993), which modulates spindles, do not explain the relationship between spindles and reasoning abilities (Fang et al., 2017). Further research is required to investigate other possible factors unrelated to sleep (e.g., age, disease, brain damage), which might mediate this relationship. Another limitation is that, when using the seed-based PPI analysis, to take a parsimonious approach, only a limited number of seed regions were chosen based on previous literature to investigate brain network connectivity during spindle events. Although beyond the scope of the current study, our future studies intend to employ whole-brain connectome approaches (e.g., graph-theoretical approach) to investigate the local and global network properties of spindles and their relationship to cognitive abilities. Finally, as would be expected from recording sleep in an MRI environment, there was substantial interparticipant variability in terms of the fast and slow spindles in the current study and a low number of events in some individuals. Therefore, it was not possible to further subdivide spindles into fast and slow spindle types without excluding participants because of missing data or insufficient number of spindle onsets (e.g., 30 events per spindle type, per participant), as some participants had a limited number for each spindle type. Thus, we did not have sufficient number of events to perform the analyses for each spindle type separately in the current study.

## CONCLUSION

In summary, we investigated the functional significance of interindividual differences in FC within the thalamo-

cortical-BG circuit and the DMN in relation to sleep spindles. Importantly, the extent of spindle-related FC in the thalamo-cortical-BG circuit was specifically associated with interindividual differences in reasoning ability but not STM or verbal abilities. For the first time, we reveal network hubs of communication, for which the strength of connectivity with other brain areas might provide insight into how sleep spindles are involved in the maintenance of normal human cognitive intellectual abilities. Furthermore, although the clinical significance and applications of the relationship between spindles and cognitive abilities has yet to be realized, this study is an important first step that may lead to the development of novel interventions utilizing spindle-enhancing neuromodulatory techniques (e.g., neurofeedback, transcranial direct current stimulation, pharmacological techniques) to improve daytime cognitive performance and explore the physiological mechanisms that support the function of sleep for memory and cognitive performance.

## Acknowledgments

This research was funded by a Canada Excellence Research Chair grant to author A. M. O. (#215063).

Reprint requests should be sent to Stuart M. Fogel, Institute for Mental Health Research, University of Ottawa, Ottawa, ON, Canada, or via e-mail: sfogel@uottawa.ca.

## UNCITED REFERENCES

Dang-Vu et al., 2008  
Möller et al., 2011

## REFERENCES

- Albouy, G., King, B. R., Maquet, P., & Doyon, J. (2013). Hippocampus and striatum: Dynamics and interaction during acquisition and sleep-related motor sequence memory consolidation. *Hippocampus*, *23*, 985–1004.
- Allen, P. J., Josephs, O., & Turner, R. (2000). A method for removing imaging artifact from continuous EEG recorded during functional MRI. *Neuroimage*, *12*, 230–239.
- Allen, P. J., Polizzi, G., Krakow, K., Fish, D. R., & Lemieux, L. (1998). Identification of EEG events in the MR scanner: The problem of pulse artifact and a method for its subtraction. *Neuroimage*, *8*, 229–239.
- Andrade, K. C., Spoormaker, V. I., Dresler, M., Wehrle, R., Holsboer, F., Sämann, P. G., et al. (2011). Sleep spindles and hippocampal functional connectivity in human NREM sleep. *Journal of Neuroscience*, *31*, 10331–10339.
- Andrillon, T., Nir, Y., Staba, R. J., Ferrarelli, F., Cirelli, C., Tononi, G., & Fried, I. (2011). Sleep spindles in humans: Insights from intracranial EEG and unit recordings. *Journal of Neuroscience*, *31*, 17821–17834.
- Baddeley, A. D. (1968). A 3 min reasoning test based on grammatical transformation. *Psychonomic Science*, *10*, 341–342.
- Bagshaw, A. P., & Khalsa, S. (2013). Functional brain imaging and consciousness. In *Neuroimaging of consciousness* (pp. 37–48). Springer.
- Baker, S. C., Rogers, R. D., Owen, A. M., Frith, C. D., Dolan, R. J., Frackowiak, R. S., et al. (1996). Neural systems engaged by

- planning: A PET study of the tower of London task. *Neuropsychologia*, *34*, 515–526.
- Beauducel, A., Brocke, B., & Liepmann, D. (2001). Perspectives on fluid and crystallized intelligence: Facets for verbal, numerical, and figural intelligence. *Personality and Individual Differences*, *30*, 977–994.
- Beck, A. T., Rial, W. Y., & Rickels, K. (1974). Short form of depression inventory: Cross-validation. *Psychological Reports*, *34*, 1184–1186.
- Beck, A. T., Steer, R. A., & Carbin, M. G. (1988). Psychometric properties of the Beck depression inventory: Twenty-five years of evaluation. *Clinical Psychology Review*, *8*, 77–100.
- Benchenane, K., Peyrache, A., Khamassi, M., Tierney, P. L., Gioanni, Y., Battaglia, F. P., et al. (2010). Coherent theta oscillations and reorganization of spike timing in the hippocampal–prefrontal network upon learning. *Neuron*, *66*, 921–936.
- Bergmann, T. O., Mölle, M., Diedrichs, J., Born, J., & Siebner, H. R. (2012). Sleep spindle-related reactivation of category-specific cortical regions after learning face–scene associations. *Neuroimage*, *59*, 2733–2742.
- Bixler, E. O., & Rhodes, J. M. (1968). Spindle activity during sleep in cultural–familial mild retardates. *Psychophysiology*, *5*, 212.
- Blumenfeld, H. (2005). Consciousness and epilepsy: Why are patients with absence seizures absent? *Progress in Brain Research*, *150*, 271–286.
- Bódizs, R., Kis, T., Lázár, A. S., Havrán, L., Rigó, P., Clemens, Z., et al. (2005). Prediction of general mental ability based on neural oscillation measures of sleep. *Journal of Sleep Research*, *14*, 285–292.
- Bódizs, R., Lázár, A. S., & Rigó, P. (2008). Correlation of visuospatial memory ability with right parietal EEG spindling during sleep. *Acta Physiologica Hungarica*, *95*, 297–306.
- Bohlken, M. M., Brouwer, R. M., Mandl, R. C., van Haren, N. E., Brans, R. G., van Baal, G. C., et al. (2014). Genes contributing to subcortical volumes and intellectual ability implicate the thalamus. *Human Brain Mapping*, *35*, 2632–2642.
- Bonjean, M., Baker, T., Bazhenov, M., Cash, S., Halgren, E., & Sejnowski, T. (2012). Interactions between core and matrix thalamocortical projections in human sleep spindle synchronization. *Journal of Neuroscience*, *32*, 5250–5263.
- Bonjean, M., Baker, T., Lemieux, M., Timofeev, I., Sejnowski, T., & Bazhenov, M. (2011). Corticothalamic feedback controls sleep spindle duration in vivo. *Journal of Neuroscience*, *31*, 9124–9134.
- Botvinick, M. M., Cohen, J. D., & Carter, C. S. (2004). Conflict monitoring and anterior cingulate cortex: An update. *Trends in Cognitive Sciences*, *8*, 539–546.
- Boutin, A., Pinsard, B., Boré, A., Carrier, J., Fogel, S. M., & Doyon, J. (2018). Transient synchronization of hippocampostriato-thalamo-cortical networks during sleep spindle oscillations induces motor memory consolidation. *Neuroimage*, *169*, 419–430.
- Boveroux, P., Vanhauzenhuysse, A., Bruno, M. A., Noirhomme, Q., Lauwick, S., Luxen, A., et al. (2010). Breakdown of within- and between-network resting state functional magnetic resonance imaging connectivity during propofol-induced loss of consciousness. *Anesthesiology*, *113*, 1038–1053.
- Branger, P., Arenaza-Urquijo, E. M., Tomadesso, C., Mézence, F., André, C., de Flores, R., et al. (2016). Relationships between sleep quality and brain volume, metabolism, and amyloid deposition in late adulthood. *Neurobiology of Aging*, *41*, 107–114.
- Braun, A. R., Balkin, T. J., Wesensten, N. J., Carson, R. E., Varga, M., Baldwin, P., et al. (1997). *Regional cerebral blood flow throughout the sleep–wake cycle: An H 215 O PET study* (pp. 1173–1197).
- Brown, P., & Marsden, C. D. (1998). What do the basal ganglia do? *Lancet*, *351*, 1801–1804.
- Cajochen, C., Münch, M., Knoblauch, V., Blatter, K., & Wirz-Juste, A. (2006). Age-related changes in the circadian and homeostatic regulation of human sleep. *Chronobiology International*, *23*, 461–474.
- Caporro, M., Haneef, Z., Yeh, H. J., Lenartowicz, A., Buttinelli, C., Parvizi, J., et al. (2012). Functional MRI of sleep spindles and K-complexes. *Clinical Neurophysiology*, *123*, 303–309.
- Carter, C. S., & van Veen, V. (2007). Anterior cingulate cortex and conflict detection: An update of theory and data. *Cognitive, Affective & Behavioral Neuroscience*, *7*, 367–379.
- Casey, B. J., Tottenham, N., Liston, C., & Durston, S. (2005). Imaging the developing brain: What have we learned about cognitive development? *Trends in Cognitive Sciences*, *9*, 104–110.
- Cattell, R. B. (1949). *Culture Free Intelligence Test, Scale 1, handbook*. Champaign, IL: Institute of Personality and Ability.
- Chen, M. C., Chiang, W.-Y., Yugay, T., Patxot, M., Özçivit, I. B., Hu, K., et al. (2016). Anterior insula regulates multiscale temporal organization of sleep and wake activity. *Journal of Biological Rhythms*, *31*, 182–193.
- Clemens, Z., Mölle, M., Eross, L., Barsi, P., Halász, P., & Born, J. (2007). Temporal coupling of parahippocampal ripples, sleep spindles and slow oscillations in humans. *Brain*, *130*, 2868–2878.
- Clemens, Z., Mölle, M., Eross, L., Jakus, R., Rásonyi, G., Halász, P., et al. (2011). Fine-tuned coupling between human parahippocampal ripples and sleep spindles. *European Journal of Neuroscience*, *33*, 511–520.
- Cohen, J. (1988). *Statistical power analysis for the behavioral sciences*. Hillsdale, NJ: Erlbaum.
- Collins, P., Roberts, A., Dias, R., Everitt, B. J., & Robbins, T. W. (1998). Perseveration and strategy in a novel spatial self-ordered sequencing task for nonhuman primates: Effects of excitotoxic lesions and dopamine depletions of the. *Journal of Cognitive Neuroscience*, *10*, 332–354.
- Coricelli, G., & Nagel, R. (2009). Neural correlates of depth of strategic reasoning in medial prefrontal cortex. *Proceedings of the National Academy of Sciences, U.S.A.*, *106*, 9163–9168.
- Corsi, P. (1972). *Human memory and the medial temporal region of the brain [PhD thesis]*. McGill University, Montreal, Canada.
- Cote, K. A., Epps, T. M., & Campbell, K. B. (2000). The role of the spindle in human information processing of high-intensity stimuli during sleep. *Journal of Sleep Research*, *9*, 19–26.
- Cox, R., van Driel, J., de Boer, M., & Talamini, L. M. (2014). Slow oscillations during sleep coordinate interregional communication in cortical networks. *Journal of Neuroscience*, *34*, 16890–16901.
- Dang-Vu, T. T., McKinney, S. M., Buxton, O. M., Solet, J. M., & Ellenbogen, J. M. (2010). Spontaneous brain rhythms predict sleep stability in the face of noise. *Current Biology*, *20*, R626–R627.
- Dang-Vu, T. T., Schabus, M., Desseilles, M., Albouy, G., Boly, M., Darsaud, A., et al. (2008). Spontaneous neural activity during human slow wave sleep. *Proceedings of the National Academy of Sciences, U.S.A.*, *105*, 15160–15165.
- Das, A., Sampson, A. L., Lainscsek, C., Muller, L., Lin, W., Doyle, J. C., et al. (2017). Interpretation of the precision matrix and its application in estimating sparse brain connectivity during sleep spindles from human electrocorticography recordings. *Neural Computation*, *29*, 603–642.
- De Gennaro, L., Ferrara, M., Vecchio, F., Curcio, G., & Bertini, M. (2005). An electroencephalographic fingerprint of human sleep. *Neuroimage*, *26*, 114–122.
- Deligianni, F., Centeno, M., Carmichael, D. W., & Clayden, J. D. (2014). Relating resting-state fMRI and EEG whole-brain

- connectomes across frequency bands. *Frontiers in Neuroscience*, 8, 258.
- Delorme, A., & Makeig, S. (2004). EEGLAB: An open source toolbox for analysis of single-trial EEG dynamics including independent component analysis. *Journal of Neuroscience Methods*, 134, 9–21.
- Destexhe, A., & Sejnowski, T. J. (2003). Interactions between membrane conductances underlying thalamocortical slow-wave oscillations. *Physiological Reviews*, 83, 1401–1453.
- Di Martino, A., Scheres, A., Margulies, D. S., Kelly, A. M. C., Uddin, L. Q., Shehzad, Z., et al. (2008). Functional connectivity of human striatum: A resting state fMRI study. *Cerebral Cortex*, 18, 2735–2747.
- Dijk, D., & Czeisler, C. (1995). Contribution of the circadian pacemaker and the sleep homeostat to sleep propensity, sleep structure, electroencephalographic slow waves, and sleep spindle activity in humans. *Journal of Neuroscience*, 15, 3526–3538.
- Dijk, D. J., Hayes, B., & Czeisler, C. A. (1993). Dynamics of electroencephalographic sleep spindles and slow wave activity in men: Effect of sleep deprivation. *Brain Research*, 626, 190–199.
- Dijk, D. J., & Cajochen, C. (1997). Melatonin and the circadian regulation of sleep initiation, consolidation, structure, and the sleep EEG. *Journal of Biological Rhythms*, 12, 627–635.
- Douglass, A. B., Bornstein, R., Nino-Murcia, G., Keenan, S., Miles, L., Zarcone, V. P., Jr., et al. (1994). The sleep disorders questionnaire. I: Creation and multivariate structure of SDQ. *Sleep*, 17, 160–167.
- Doyon, J., Bellec, P., Amsel, R., Penhune, V., Monchi, O., Carrier, J., et al. (2009). Contributions of the basal ganglia and functionally related brain structures to motor learning. *Behavioural Brain Research*, 199, 61–75.
- Doyon, J., & Benali, H. (2005). Reorganization and plasticity in the adult brain during learning of motor skills. *Current Opinion in Neurobiology*, 15, 161–167.
- Doyon, J., Korman, M., Morin, A., Dostie, V., Hadj Tahar, A., Benali, H., et al. (2009). Contribution of night and day sleep vs. simple passage of time to the consolidation of motor sequence and visuomotor adaptation learning. *Experimental Brain Research*, 195, 15–26.
- Doyon, J., & Ungerleider, L. G. (2002). Functional anatomy of motor skill learning. *Neuropsychology of Memory*, 3, 225–238.
- Duncan, J. (2000). A neural basis for general intelligence. *Science*, 289, 457–460.
- Elton, M., Winter, O., Heslenfeld, D., Loewy, D., Campbell, K., & Kok, A. (1997). Event-related potentials to tones in the absence and presence of sleep spindles. *Journal of Sleep Research*, 6, 78–83.
- Fair, D. A., Cohen, A. L., Dosenbach, N. U., Church, J. A., Miezin, F. M., Barch, D. M., et al. (2008). The maturing architecture of the brain's default network. *Proceedings of the National Academy of Sciences, U.S.A.*, 105, 4028–4032.
- Fang, Z., Ray, L. B., Owen, A. M., & Fogel, S. M. (2019). Brain activation time-locked to sleep spindles associated with human cognitive abilities. *Frontiers in Neuroscience*, 13, 46.
- Fang, Z., Sergeeva, V., Ray, L. B., Viczko, J., Owen, A. M., & Fogel, S. M. (2017). Sleep spindles and intellectual ability: Epiphenomenon or directly related? *Journal of Cognitive Neuroscience*, 29, 167–182.
- Faul, F., Erdfelder, E., Buchner, A., & Lang, A. G. (2009). Statistical power analyses using G\*Power 3.1: Tests for correlation and regression analyses. *Behavior Research Methods*, 41, 1149–1160.
- Faul, F., Erdfelder, E., Lang, A.-G., & Buchner, A. (2007). GPOWER: A general power analysis program. *Behavior Research Methods*, 39, 175–191.
- Fogel, S., Albouy, G., King, B. R., Lungu, O., Vien, C., Bore, A., et al. (2017). Reactivation or transformation? Motor memory consolidation associated with cerebral activation time-locked to sleep spindles. *PLoS One*, 12, 1–26.
- Fogel, S., Albouy, G., Vien, C., Popovici, R., King, B. R., Hoge, R. D., et al. (2014). fMRI and sleep correlates of the age-related impairment in motor memory consolidation. *Human Brain Mapping*, 35, 3625–3645.
- Fogel, S., Nader, R. S., Cote, K. A., & Smith, C. (2007). Sleep spindles and learning potential. *Behavioral Neuroscience*, 121, 1–10.
- Fogel, S., & Smith, C. T. (2006). Learning-dependent changes in sleep spindles and Stage 2 sleep. *Journal of Sleep Research*, 15, 250–255.
- Fogel, S., Vien, C., Karni, A., Benali, H., Carrier, J., & Doyon, J. (2017). Sleep spindles: A physiological marker of age-related changes in gray matter in brain regions supporting motor skill memory consolidation. *Neurobiology of Aging*, 49, 154–164.
- Folstein, M. F., Folstein, S. E., & McHugh, P. R. (1975). Minimal state. *Journal of Psychiatric Research*, 12, 189–198.
- Friston, K. J., Williams, S., Howard, R., Frackowiak, R. S., & Turner, R. (1996). Movement-related effects in fMRI time-series. *Magnetic Resonance in Medicine*, 35, 346–355.
- Gibbs, E. L., & Gibbs, F. A. (1962). Extreme spindles: Correlation of electroencephalographic sleep pattern with mental retardation. *Science*, 138, 1106–1107.
- Girardeau, G., & Zugaro, M. (2011). Hippocampal ripples and memory consolidation. *Current Opinion in Neurobiology*, 21, 452–459.
- Gong, Q. Y., Sluming, V., Mayes, A., Keller, S., Barrick, T., Cezayirli, E., et al. (2005). Voxel-based morphometry and stereology provide convergent evidence of the importance of medial prefrontal cortex for fluid intelligence in healthy adults. *Neuroimage*, 25, 1175–1186.
- Gould, R. L., Brown, R. G., Owen, A. M., Bullmore, E. T., & Howard, R. J. (2006). Task-induced deactivations during successful paired associates learning: An effect of age but not Alzheimer's disease. *Neuroimage*, 31, 818–831.
- Gray, J. R., Chabris, C. F., & Braver, T. S. (2003). Neural mechanisms of general fluid. *Nature Neuroscience*, 6, 316–322.
- Hampshire, A., Highfield, R. R., Parkin, B. L., & Owen, A. M. (2012). Fractionating human intelligence. *Neuron*, 76, 1225–1237.
- Hayasaka, S., Phan, K. L., Liberzon, I., Worsley, K. J., & Nichols, T. E. (2004). Nonstationary cluster-size inference with random field and permutation methods. *Neuroimage*, 22, 676–687.
- Heine, L., Soddu, A., Gómez, F., Vanhauzenhuyse, A., Tshibanda, L., Thonnard, M., et al. (2012). Resting state networks and consciousness Alterations of multiple resting state network connectivity in physiological, pharmacological, and pathological consciousness states. *Frontiers in Psychology*, 3, 295.
- Herweg, N. A., Apitz, T., Leicht, G., Mulert, C., Fuentemilla, L., & Bunzeck, N. (2016). Theta-alpha oscillations bind the hippocampus, prefrontal cortex, and striatum during recollection: Evidence from simultaneous EEG-fMRI. *Journal of Neuroscience*, 36, 3579–3587.
- Horne, J. A., & Ostberg, O. (1976). A self-assessment questionnaire to determine morningness–eveningness in human circadian rhythms. *International Journal of Chronobiology*, 4, 97–110.
- Horowitz, S. G., Braun, A. R., Carr, W. S., Picchioni, D., Balkin, T. J., Fukunaga, M., et al. (2009). Decoupling of the brain's default mode network during deep sleep. *Proceedings of the National Academy of Sciences, U.S.A.*, 106, 11376–11381.

- Horowitz, S. G., Fukunaga, M., de Zwart, J. A., van Gelderen, P., Fulton, S. C., Balkin, T. J., et al. (2008). Low frequency BOLD fluctuations during resting wakefulness and light sleep: A simultaneous EEG-fMRI study. *Human Brain Mapping, 29*, 671–682.
- Houdin, E., Fang, Z., Ray, L. B., Owen, A. M., & Fogel, S. M. (2019). Toward a complete taxonomy of resting state networks across wakefulness and sleep: An assessment of spatially distinct resting state networks using independent component analysis. *Sleep, 42*, 1–9.
- Iber, C., Ancoli-Israel, S., Chesson, A. L., & Quan, S. F. (2007). *The AASM manual for the scoring of sleep and associated events: Rules, terminology and technical specifications*. Westchester, IL: American Academy of Sleep Medicine.
- Inoue, S., & Matsuzawa, T. (2007). Working memory of numerals in chimpanzees. *Current Biology, 17*, R1004–R1005.
- Jackson, D. (1998). *Multidimensional Aptitude Battery-II manual*.
- Jegou, A., Schabus, M., Gosseries, O., Dahmen, B., Albouy, G., Desseilles, M., et al. (2019). Cortical reactivations during sleep spindles following declarative learning. *Neuroimage, 195*, 104–112.
- Jia, X., Liang, P., Lu, J., Yang, Y., Zhong, N., & Li, K. (2011). Common and dissociable neural correlates associated with component processes of inductive reasoning. *Neuroimage, 56*, 2292–2299.
- Kalbfleisch, M. L., Van Meter, J. W., & Zeffiro, T. A. (2007). The influences of task difficulty and response correctness on neural systems supporting fluid reasoning. *Cognitive Neurodynamics, 1*, 71–84.
- Kanazawa, S. (2004). General intelligence as a domain-specific adaptation. *Psychological Review, 111*, 512.
- Knoblauch, V., Martens, W., Wirz-Justice, A., Kräuchi, K., & Cajochen, C. (2003). Regional differences in the circadian modulation of human sleep spindle characteristics. *European Journal of Neuroscience, 18*, 155–163.
- Knoblauch, V., Münch, M., Blatter, K., Martens, W. L., Schröder, C., Schnitzler, C., et al. (2005). Age-related changes in the circadian modulation of sleep-spindle frequency during nap sleep. *Sleep, 28*, 1093–1101.
- Koike, T., Kan, S., Misaki, M., & Miyauchi, S. (2011). Connectivity pattern changes in default-mode network with deep non-REM and REM sleep. *Neuroscience Research, 69*, 322–330.
- Kouneiher, F., Charron, S., & Koechlin, E. (2009). Motivation and cognitive control in the human prefrontal cortex. *Nature Neuroscience, 12*, 939–945.
- Larson-Prior, L. J., Zempel, J. M., Nolan, T. S., Prior, F. W., Snyder, A. Z., & Raichle, M. E. (2009). Cortical network functional connectivity in the descent to sleep. *Proceedings of the National Academy of Sciences, U.S.A., 106*, 4489–4494.
- Laufs, H., Walker, M. C., & Lund, T. E. (2007). Brain activation and hypothalamic functional connectivity during human non-rapid eye movement sleep: An EEG/fMRI study—Its limitations and an alternative approach. *Brain, 130*, e75.
- Laureys, S. (2005). The neural correlate of (un)awareness: Lessons from the vegetative state. *Trends in Cognitive Sciences, 9*, 556–559.
- Lehéricy, S., Benali, H., Van de Moortele, P. F., Pélégriani-Issac, M., Waechter, T., Ugurbil, K., et al. (2005). Distinct basal ganglia territories are engaged in early and advanced motor sequence learning. *Proceedings of the National Academy of Sciences, U.S.A., 102*, 12566–12571.
- Lehéricy, S., Ducros, M., Krainik, A., Francois, C., de Moortele, P. F., Ugurbil, K., et al. (2004). 3-D diffusion tensor axonal tracking shows distinct SMA and pre-SMA projections to the human striatum. *Cerebral Cortex, 14*, 1302–1309.
- Liang, P., Jia, X., Taatgen, N. A., Zhong, N., & Li, K. (2014). Different strategies in solving series completion inductive reasoning problems: An fMRI and computational study. *International Journal of Psychophysiology, 93*, 253–260.
- Luthi, A. (2014). Sleep spindles: Where they come from, what they do. *Neuroscientist, 20*, 243–256.
- MacDonald, A. A., Naci, L., MacDonald, P. A., & Owen, A. M. (2015). Anesthesia and neuroimaging: Investigating the neural correlates of unconsciousness. *Trends in Cognitive Sciences, 19*, 100–107.
- Mantini, D., Perrucci, M. G., Cugini, S., Ferretti, A., Romani, G. L., & Del Gratta, C. (2007). Complete artifact removal for EEG recorded during continuous fMRI using independent component analysis. *Neuroimage, 34*, 598–607.
- Martuzzi, R., Ramani, R., Qiu, M., Rajeevan, N., & Constable, R. T. (2010). Functional connectivity and alterations in baseline brain state in humans. *Neuroimage, 49*, 823–834.
- McLaren, D. G., Ries, M. L., Xu, G., & Johnson, S. C. (2012). A generalized form of context-dependent psychophysiological interactions (gPPI): A comparison to standard approaches. *Neuroimage, 4*, 1277–1286.
- Melrose, R. J., Poulin, R. M., & Stern, C. E. (2007). An fMRI investigation of the role of the basal ganglia in reasoning. *Brain Research, 2*, 146–158.
- Morin, A., Doyon, J., Dostie, V., Barakat, M., Hadj Tahar, A., Korman, M., et al. (2008). Motor sequence learning increases sleep spindles and fast frequencies in post-training sleep. *Sleep, 31*, 1149–1156.
- Mölle, M., Bergmann, T. O., Marshall, L., & Born, J. (2011). Fast and slow spindles during the sleep slow oscillation: Disparate coalescence and engagement in memory processing. *Sleep, 34*, 1411–1421.
- Mulert, C., & Lemieux, L. (Eds.) (2009). *EEG-fMRI: Physiological basis, technique, and applications*. Springer.
- Mullinger, K. J., Yan, W. X., & Bowtell, R. (2011). Reducing the gradient artefact in simultaneous EEG-fMRI by adjusting the subject's axial position. *Neuroimage, 54*, 1942–1950.
- Murphy, M., Riedner, B. A., Huber, R., Massimini, M., Ferrarelli, F., & Tononi, G. (2009). Source modeling sleep slow waves. *Proceedings of the National Academy of Sciences, U.S.A., 106*, 1608–1613.
- Nader, R. S., & Smith, C. (2001). The relationship between stage 2 sleep spindles and intelligence. *Sleep, 24*, A160.
- Nader, R. S., & Smith, C. (2003). A role for Stage 2 sleep in memory processing. *Sleep and Brain Plasticity, 1*, 87–99.
- Peters, A., & Jones, E. G. (Eds.). (1991). *Normal and altered states of function*. <https://doi.org/10.1007/978-1-4615-6622-9>
- Peyrache, A., Battaglia, F. P., & Destexhe, A. (2011). Inhibition recruitment in prefrontal cortex during sleep spindles and gating of hippocampal inputs. *Proceedings of the National Academy of Sciences, U.S.A., 108*, 17207–17212.
- Picchioni, D., Duyn, J. H., & Horowitz, S. G. (2013). Sleep and the functional connectome. *Neuroimage, 80*, 387–396.
- Picchioni, D., Pixa, M. L., Fukunaga, M., Carr, W. S., Horowitz, S. G., Braun, A. R., et al. (2014). Decreased connectivity between the thalamus and the neocortex during human nonrapid eye movement sleep. *Sleep, 37*, 387–397.
- Price, A. L. (2005). Cortico-striatal contributions to category learning: Dissociating the verbal and implicit systems. *Behavioral Neuroscience, 119*, 1438–1447.
- Purpura, D. (1968). Brain reflexes. In *Proceedings of the International Conference dedicated to the centenary celebration of the publication of I. M. Sechenov's book Brain Reflexes*. Progress in Brain Research. [https://doi.org/10.1016/S0079-6123\(08\)63499-8](https://doi.org/10.1016/S0079-6123(08)63499-8).
- Ray, L. B., Sockeel, S., Soon, M., Bore, A., Myhr, A., Stojanoski, B., et al. (2015). Expert and crowd-sourced validation of an individualized sleep spindle detection method employing complex demodulation and individualized normalization. *Frontiers in Human Neuroscience, 9*, 507.

- Rodriguez-Moreno, D., & Hirsch, J. (2009). The dynamics of deductive reasoning: An fMRI investigation. *Neuropsychologia*, *47*, 949–961.
- Rybakowski, J. K., Borkowska, A., Czerni, P. M., Kapelski, P., Dmitrzak-Weglaz, M., & Hauser, J. (2005). An association study of dopamine receptors polymorphisms and the Wisconsin Card Sorting Test in schizophrenia. *Journal of Neural Transmission*, *112*, 1575–1582.
- Saletin, J. M., van der Helm, E., & Walker, M. P. (2013). Structural brain correlates of human sleep oscillations. *Neuroimage*, *83*, 658–668.
- Salthouse, T. A., Pink, J. E., & Tucker-Drob, E. M. (2008). Contextual analysis of fluid intelligence. *Intelligence*, *36*, 464–486.
- Sämman, P. G., Wehrle, R., Hoehn, D., Spoomaker, V. I., Peters, H., Tully, C., et al. (2011). Development of the brain's default mode network from wakefulness to slow wave sleep. *Cerebral Cortex*, *21*, 2082–2093.
- Schabus, M., Dang-Vu, T. T., Albouy, G., Balteau, E., Boly, M., Carrier, J., et al. (2007). Hemodynamic cerebral correlates of sleep spindles during human non-rapid eye movement sleep. *Proceedings of the National Academy of Sciences, U.S.A.*, *104*, 13164–13169.
- Schabus, M., Dang-Vu, T. T., Heib, D. P., Boly, M., Desseilles, M., Vandewalle, G., et al. (2012). The fate of incoming stimuli during NREM sleep is determined by spindles and the phase of the slow oscillation. *Frontiers in Neurology*, *3*, 40.
- Schabus, M., Hödlmoser, K., Gruber, G., Sauter, C., Anderer, P., Klösch, G., et al. (2006). Sleep spindle-related activity in the human EEG and its relation to general cognitive and learning abilities. *European Journal of Neuroscience*, *23*, 1738–1746.
- Schipolowski, S., Wilhelm, O., & Schroeders, U. (2014). On the nature of crystallized intelligence: The relationship between verbal ability and factual knowledge. *Intelligence*, *46*, 156–168.
- Selya, A. S., Rose, J. S., Dierker, L. C., Hedeker, D., & Mermelstein, R. J. (2012). A practical guide to calculating Cohen's  $f^2$ , a measure of local effect size, from PROC MIXED. *Frontiers in Psychology*, *3*, 111.
- Shallice, T. (1982). Specific impairments of planning. *Philosophical Transactions of the Royal Society: Series B: Biological Sciences*, *298*, 199–209.
- Sheffield, J. M., & Barch, D. M. (2016). Cognition and resting-state functional connectivity in schizophrenia. *Neuroscience & Biobehavioral Reviews*, *61*, 108–120.
- Shibagaki, M., & Kiyono, S. (1983). Duration of spindle bursts during nocturnal sleep in mentally retarded children. *Electroencephalography and Clinical Neurophysiology*, *55*, 645–651.
- Siapas, A. G., & Wilson, M. A. (1998). Coordinated interactions between hippocampal ripples and cortical spindles during slow-wave sleep. *Neuron*, *21*, 1123–1128.
- Silverman, I., Choi, J., Mackewn, A., Fisher, M., Moro, J., & Olshansky, E. (2000). Evolved mechanisms underlying wayfinding. *Evolution and Human Behavior*, *21*, 201–213.
- Silverstein, L. D., & Levy, C. M. (1976). The stability of the sigma sleep spindle. *Electroencephalography and Clinical Neurophysiology*, *40*, 666–670.
- Spoomaker, V. I., Schröter, M. S., Gleiser, P. M., Andrade, K. C., Dresler, M., Wehrle, R., et al. (2010). Development of a large-scale functional brain network during human non-rapid eye movement sleep. *Journal of Neuroscience*, *30*, 11379–11387.
- Srivastava, G., Cottazz-Herbette, S., Lau, K. M., Glover, G. H., & Menon, V. (2005). ICA-based procedures for removing ballistocardiogram artifacts from EEG data acquired in the MRI scanner. *Neuroimage*, *24*, 50–60.
- Steriade, M. (2006). Grouping of brain rhythms in corticothalamic systems. *Neuroscience*, *137*, 1087–1106.
- Steriade, M., Domich, L., Oakson, G., & Deschênes, M. (1987). The deafferented reticular thalamic nucleus generates spindle rhythmicity. *Journal of Neurophysiology*, *57*, 260–273.
- Steriade, M., McCormick, D. A., & Sejnowski, T. J. (1993). Thalamocortical oscillations in the sleeping and aroused brain. *Science*, *262*, 679–685.
- Steriade, M., Nuñez, A., & Amzica, F. (1993). A novel slow (< 1 Hz) oscillation of neocortical neurons in vivo: Depolarizing and hyperpolarizing components. *Journal of Neuroscience*, *13*, 3252–3265.
- Sternberg, R. J., Conway, B. E., Ketron, J. L., & Bernstein, M. (1981). People's conceptions of intelligence. *Journal of Personality and Social Psychology*, *41*, 37.
- Stroop, J. R. (1935). Studies of interference in serial verbal reactions. *Journal of Experimental Psychology*, *18*, 643.
- Tagliazucchi, E., & Laufs, H. (2014). Decoding wakefulness levels from typical fMRI resting-state data reveals reliable drifts between wakefulness and sleep. *Neuron*, *82*, 695–708.
- Tagliazucchi, E., & van Someren, E. J. W. (2017). The large-scale functional connectivity correlates of consciousness and arousal during the healthy and pathological human sleep cycle. *Neuroimage*, *160*, 55–72.
- Timofeev, I. (2001). Contribution of intrinsic and synaptic factors in the desynchronization of thalamic oscillatory activity. *Thalamus & Related Systems*, *1*, 53–69.
- Tranter, L. J., & Koutstaal, W. (2008). Age and flexible thinking: An experimental demonstration of the beneficial effects of increased cognitively stimulating activity on fluid intelligence in healthy older adults. *Aging, Neuropsychology, and Cognition*, *15*, 184–207.
- Treisman, A. M., & Gelade, G. (1980). A feature-integration theory of attention. *Cognitive Psychology*, *12*, 97–136.
- Tyvaert, L., Levan, P., Grova, C., Dubeau, F., & Gotman, J. (2008). Clinical neurophysiology effects of fluctuating physiological rhythms during prolonged EEG-fMRI studies. *Clinical Neurophysiology*, *119*, 2762–2774.
- Ujma, P. P., Bódizs, R., Gombos, F., Stintzing, J., Konrad, B. N., Genzel, L., et al. (2015). Nap sleep spindle correlates of intelligence. *Scientific Reports*, *5*, 17159.
- Ujma, P. P., Konrad, B. N., Genzel, L., Bleifuss, A., Simor, P., Pótári, A., et al. (2014). Sleep spindles and intelligence: Evidence for a sexual dimorphism. *Journal of Neuroscience*, *34*, 16358–16368.
- Ullsperger, M., & von Cramon, D. Y. (2004). Neuroimaging of performance monitoring: Error detection and beyond. *Cortex*, *40*, 593–604.
- Vahdat, S., Fogel, S., Benali, H., & Doyon, J. (2017). Network-wide reorganization of procedural memory during NREM sleep revealed by fMRI. *ELife*, *6*, 1–24.
- Vanhoudenhuyse, A., Noirhomme, Q., Tshibanda, L. J. F., Bruno, M. A., Boveroux, P., Schnakers, C., et al. (2010). Default network connectivity reflects the level of consciousness in non-communicative brain-damaged patients. *Brain*, *133*, 161–171.
- von Krosigk, M., Bal, T., & McCormick, D. A. (1993). Cellular mechanisms of a synchronized oscillation in the thalamus. *Science*, *261*, 361–364.
- Vyazovskiy, V. V., Achermann, P., Borbély, A. A., & Tobler, I. (2004). The dynamics of spindles and EEG slow-wave activity in NREM sleep in mice. *Archives Italiennes de Biologie*, *142*, 511–523.
- Waltz, J. A., Knowlton, B. J., Holyoak, K. J., Boone, K. B., Mishkin, F. S., de Menezes Santos, M., et al. (1999). A system for relational reasoning in human prefrontal cortex. *Psychological Science*, *10*, 119–125.

- Wechsler, D. A. (1981). *Wechsler Adult Intelligence Scale–Revised (WAIS-R)*. New York, NY: The Psychological Corporation.
- Weinberger, D. R., Berman, K. F., Suddath, R., & Torrey, E. F. (1992). Evidence of dysfunction of a prefrontal-limbic network in schizophrenia: A magnetic resonance imaging and regional cerebral blood flow study of discordant monozygotic twins. *American Journal of Psychiatry*, *149*, 890–897.
- Wild, C. J., Nichols, E. S., Battista, M. E., Stojanoski, B., & Owen, A. M. (2018). Dissociable effect of self-reported daily sleep duration on high-level cognitive abilities. *Sleep*, *12*, 1–11.
- Wirsich, J., Ridley, B., Besson, P., Jirsa, V., Bénar, C., Ranjeva, J. P., et al. (2017). Complementary contributions of concurrent EEG and fMRI connectivity for predicting structural connectivity. *Neuroimage*, *161*, 251–260.
- Yan, C., & Zang, Y. (2010). DPARSF: A MATLAB toolbox for “pipeline” data analysis of resting-state fMRI. *Frontiers in Systems Neuroscience*, *4*, 13.
- Yuan, Z., Qin, W., Wang, D., Jiang, T., Zhang, Y., & Yu, C. (2012). The salience network contributes to an individual’s fluid reasoning capacity. *Behavioural Brain Research*, *229*, 384–390.
- Zerouali, Y., Lina, J. M., Sekerovic, Z., Godbout, J., Dube, J., Jolicoeur, P., et al. (2014). A time–frequency analysis of the dynamics of cortical networks of sleep spindles from MEG-EEG recordings. *Frontiers in Neuroscience*, *8*, 310.

Uncorrected Proof